OCEAN
ISSN 3008-1203
Open Access
Review Article

Wind-assisted propulsion systems for green shipping: A techno-economic review

Wenzhe Zhang[1] ✉, Zhiyu Jiang[2], Javier Calderon-Sanchez[1], Lisa Martínez[3], Simone Saettone[3], H. Bill Galdós-Lindao[4], and Jordi Mas-Soler[4]

[1] CEHINAV, DACSON, Escuela Técnica Superior de Ingeniería Naval, Universidad Politécnica de Madrid, Madrid 28040, Spain
[2] Department of Engineering Sciences, University of Agder, Grimstad, Norway
[3] Bound4blue, San Cugat, Barcelona, Spain
[4] Naval Arch. & Ocean Eng. Department, Escola Politécnica da Universidade de São Paulo, São Paulo, Brazil

Cite This: *Ocean*, **2026**, *2*, 9470019

Read Online

ABSTRACT: Wind-assisted propulsion systems (WAPSs) are emerging and promising technologies for maritime decarbonization. Although WAPSs have witnessed rapid growth and commercial deployment in recent years, several challenges remain such as its inadequate propulsion efficiency, uncertain operational safety, insufficient economic assessment, and lack of standards and policy frameworks. The implementation of WAPSs is inherently multidisciplinary, with key concerns centered on safety, efficiency, and cost. To address these concerns, a state-of-the-art review of scientific research, industrial developments, and life cycle impact assessments of WAPSs is presented herein. Four types of WAPSs, namely rotor, boundary-layer control, wing, and kite sails, are classified and defined. This review covers critical aspects, including industrial and academic developments, unit aerodynamic characteristics, design procedure and considerations, operational challenges, and environmental, economic, social, and political impacts of WAPS deployment. Key limitations and challenges are also discussed, and nine critical future research directions are outlined. This review aims to provide a reference for guiding the safe, efficient, and cost-effective integration of WAPSs into green shipping.

KEYWORDS: wind-assisted propulsion, green shipping, decarbonization, offshore wind energy, maritime transportation

1 Introduction

Carbon neutrality is a fundamental global objective for mitigating climate change [1,2]. Maritime transport accounts for ~3% of global anthropogenic greenhouse gas (GHG) emissions and this proportion is projected to increase in the future [3]. Therefore, the maritime sector is a critical component in achieving carbon neutrality. In response to growing environmental concerns, this industry is subject to increasingly stringent regulations aimed at achieving green shipping with low- or zero GHG emissions.

Globally, the International Maritime Organization (IMO) has been actively working to reduce GHG emissions from shipping by implementing various regulatory measures. These include the adoption of the global Net-Zero Framework, the enforcement of the Energy Efficiency Design Index for newly built ships and the Ship Energy Efficiency Management Plan (SEEMP) since 2013, the development of the IMO Data Collection System to support policy-making since 2016, the Energy Efficiency Existing Ship Index (EEXI) requirements for pre-2013 vessels and the Carbon Intensity Indicator (CII) for all operating vessels over 5000 gross tonnage since 2023. The IMO has also set ambitious GHG emission reduction targets. A reduction in carbon intensity by at least 40% by 2030 relative to 2008 levels, with zero or near-zero-emission technologies accounting for 5%–10% of total shipping energy consumption; and achieving a 70%–80% reduction in total emissions relative to 2008 levels, ultimately reaching net-zero emissions by 2050 [4]. The timeline of major IMO regulations is shown in Fig. 1.

In addition to global governance, regional institutions such as the European Union (EU) are promoting maritime decarbonization initiatives by introducing the EU Emissions Trading System (EU ETS) and the FuelEU Maritime Regulation (FuelEU). The EU ETS incorporated maritime transportation in 2024, implementing a cap-and-trade mechanism that assigns a financial cost to CO_2 emissions and incentivizing ship operators to adopt energy-efficient technologies. FuelEU took effect in 2025 and gradually tightened the GHG intensity limits of marine fuels, starting with a 2% reduction in 2025 and aiming for an 80% reduction by 2050 [5]. Those regulations collectively promote the adoption of green maritime transportation. A comparative timeline of important EU regulations is given in Fig. 1.

Against this environmental and political background, numerous technologies have been proposed to achieve the objective of zero-emission shipping [6]; these include advancements in ship hull design [7,8], biofouling management [9,10], speed management [11–13], route and voyage optimization [11,14,15], exhaust gas treatment [16–18], waste heat recovery [19–21], electric propulsion [22–24], energy system optimization [25–27], and renewable energy utilization [28,29]. Among these sustainable solutions, renewable energy utilization has been garnering increasing attention across both academia and industry. This is because it directly addresses emissions at their source and represents a major

Received: September 26, 2025; **Revised:** January 12, 2026
Accepted: February 14, 2026

✉Address correspondence to Wenzhe Zhang, wenzhe.z@upm.es

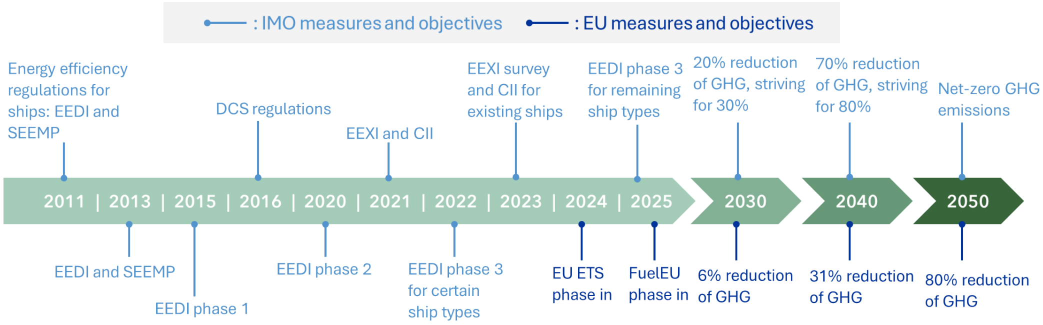

Figure 1 Important IMO and EU regulatory actions aimed at reducing GHG emissions from shipping.

shift toward greener maritime transport, supported by its high social acceptance and technological maturity. Existing renewable energy applications in shipping include solar power [28], hydrogen [30], fuel cells [31], and wind energy [32]. A key advantage of wind and solar energy is their natural availability, which eliminates the need for energy-intensive production, storage, or conversion processes required by hydrogen and fuel cells. Traditionally, these renewable sources have been primarily used for onboard electricity generation as auxiliary power.

Recent advancements have enabled the use of wind-assisted propulsion systems (WAPSs) as an application of renewable energy. WAPSs convert wind energy directly into propulsive thrust, thereby improving fuel efficiency and reducing emissions without intermediary energy storage. Although the maximum decarbonization potential of WAPSs is lower than that of some alternative green fuels [6], WAPSs offer a distinct advantage in terms of retrofit feasibility [33]. These systems can be integrated into existing vessels without making substantial modifications to the engine system or extensively redesigning new builds, making it a practical solution for meeting near-term carbon reduction targets. Their inherent operational safety and adaptability with conventional propulsion systems have enhanced their acceptability among shipowners and maritime sector.

Although WAPSs are being widely employed across industries, their comprehensive scholarly analyses remain scarce. This review aims to address this gap by offering a systematic and multidimensional assessment of recent developments in WAPSs. It presents an in-depth evaluation of major WAPS technologies, analyzing their performance, technical challenges, as well as associated economic and environmental impacts. This review also highlights current limitations and outline potential research directions to guide future studies in this evolving field.

This review answers several key research questions: 1) How can WAPSs be systematically categorized according to their operating principles? 2) What are the current trajectories in both academic research and industrial deployment of WAPSs? 3) What are the procedures and key considerations in WAPS design? 4) What new challenges arise during WAPS operation? 5) What benefits do WAPS bring to the economy and the environment? This paper is organized as follows: Section 1 outlines the background of and motivation for maritime decarbonization; Section 2 provides the current academic and industrial status of WAPSs; Section 3 introduces the aerodynamic characteristics of a WAPS unit; Section 4 summarizes the design procedure and associated challenges; Section 5 covers the evaluation of the operational concerns of ships caused by the integration of WAPSs; Section 6 describes the analysis of WAPS impact from environmental, economic, social, and political perspectives; Section 7 covers the future outlook; and Section 8 concludes the paper.

2 Academic research and industrial development of WAPSs

This section outlines the definition and classification framework adopted in this review, followed by a brief overview of current academic research trends and industrial application developments.

2.1 History of wind-assisted shipping

Wind has powered maritime transport for over five millennia [34]. Sailing vessel designs have evolved continuously to serve commercial, colonial, and military purposes, as illustrated in Fig. 2. This century-long dominance of wind propulsion ended abruptly during the late 19th century when steam engines and internal combustion engines displaced sails almost entirely from commercial shipping, relegating to recreational sailing fueled by events such as the America's Cup.

The recent resurgence of WAPSs represents a fundamental technological evolution rather than a simple revival of historical sailing practices. The transition from sail to steam in the late 19th century was driven by the need for schedule reliability; however, intermittent attempts to reintroduce wind power in the 20th century failed to gain traction due to low fuel prices and increased operational complexities.

However, the technological landscape has shifted dramatically since 2010. In contrast to historical vessels that relied on wind as the primary power source, modern WAPSs function as auxiliary systems designed for seamless integration with conventional propulsion. This paradigm shift is catalyzed by three modern factors: stringent IMO decarbonization regulations, advancements in automation and aerodynamics, and the economic necessity of fuel efficiency. Current WAPSs leverage historical aerodynamic principles but implement them via autonomous control systems that require minimal crew intervention. Understanding this transition from labor-intensive sailing to automated auxiliary support offers the necessary context for specific WAPS technologies and operational strategies analyzed in subsequent sections.

2.2 Technical definition and categorization of modern WAPSs

Modern WAPSs are integrated propulsion-assist technologies that capture and utilize wind energy to generate auxiliary thrust for large commercial vessels. Unlike systems that convert wind energy into electricity for shipping (e.g., vertical-axis wind turbines [38]), WAPSs utilize aerodynamic forces directly for propulsion and avoid intermediate energy conversions. The primary objective of WAPSs is to reduce dependence on fossil fuel-based propulsion, thereby lowering GHG emissions and fuel consumption. By converting wind energy into thrust via specialized aerodynamic devices, WAPSs operate synergistically with the main propulsion system of vessels (e.g., diesel engines) for enhancing the overall energy efficiency and reducing GHG emissions.

The classification of WAPSs varies across maritime institutions, European Maritime Safety Agency (EMSA) [39], Lloyd's Register (LR) [40], Det Norske Veritas (DNV) [41], and American Bureau of Shipping (ABS) [42]. In this review, current WAPSs were classified into four main types based on their distinct working principles: rotor sails, boundary-layer control (BLC) sails, wing sails, and kite sails. This framework will be the basis of subsequent reviews. Table 1 compares these classifications across institutions, and Fig. 3 schematizes each form.

Rotor sails are vertical rotating cylinders equipped with endplates at the top driven by electric motors. These motors generate thrust via the Magnus effect, as shown in Fig. 3a. BLC sails (Fig. 3b) are characterized by their vertical structures equipped with BLC mechanisms, typically implemented via internal fans or other active flow-control devices. These sails are commonly referred to as "turbosails" or "suction wings" and have been referred to as "BLC sails" in subsequent discussions. Wing sails, the most traditional

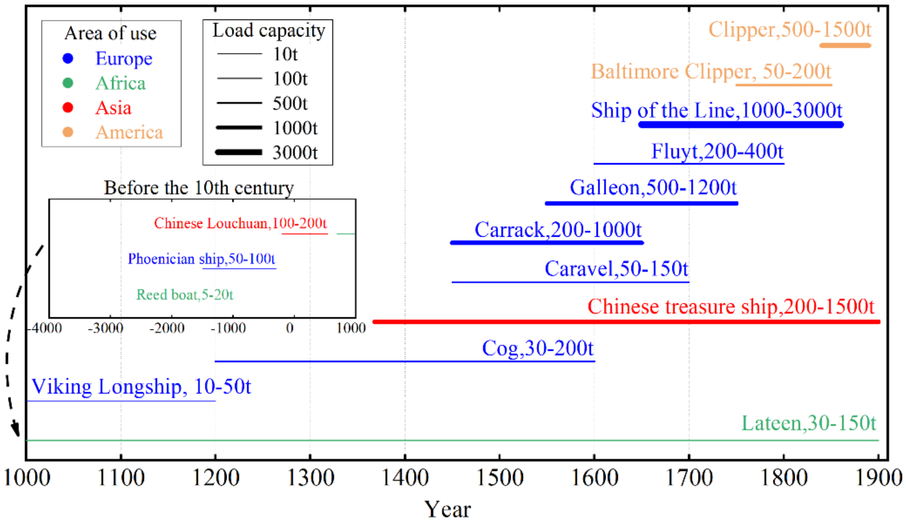

Figure 2 Brief history of wind sail [35–37].

Table 1 WAPS categorizations across different institutions

Present review	EMSA [39]	LR [40]	DNV [41]	ABS [42]
Rotor sails	Rotor sails	Flettner rotors	Rotor sails	Flettner rotors
BLC sails	Suction wings	Suction wings	Suction sails	Suction wing sails
Wing sails	Hard sails Soft sails	Rigid sails	Wing sails Soft sails	Rigid wing sails Soft wing sails
Kite sails	Kites	Kite sails	Kites	Towing kites

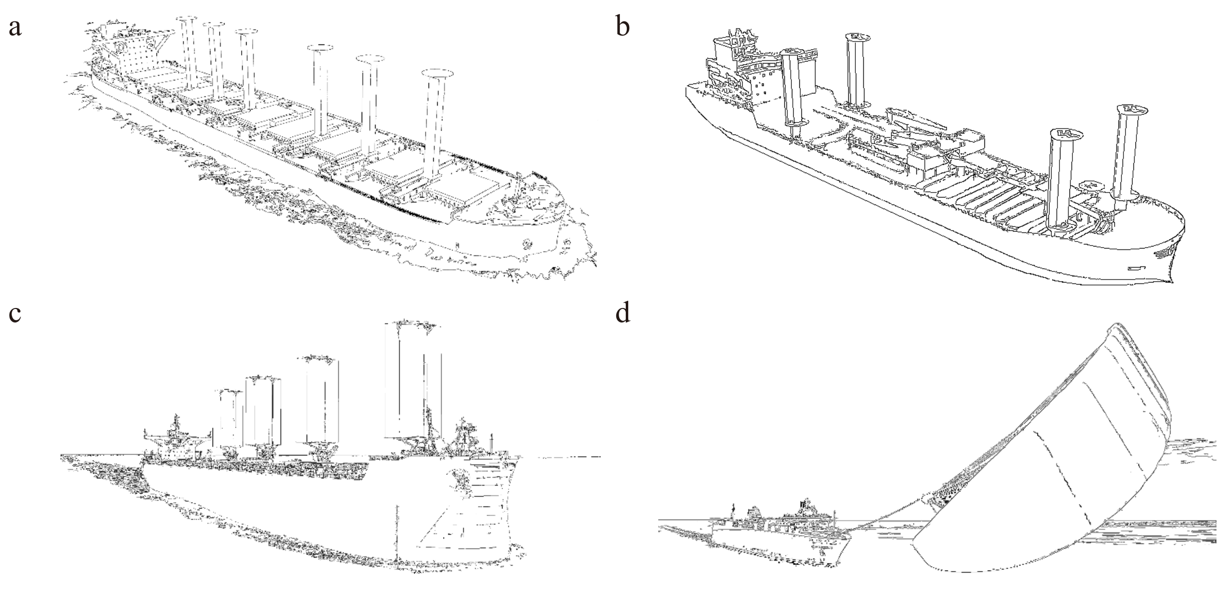

Figure 3 Schematic of four WAPS forms. (a) Rotor sails. (b) BLC sails. (c) Wing sails. (d) Kite sails.

form of WAPSs, are shown in Fig. 3c. Modern wing sails can be broadly categorized into two types based on their structural materials: hard and soft wing sails. Hard wing sails are generally more efficient and thus more commonly adopted in current large-scale commercial vessel projects, whereas soft wing sails remain limited in practical applications [39]. Kite sails, as shown in Fig. 3d, are typically installed at the bow and generate towing force by harnessing strong and stable winds at high altitudes. Their main advantage is the efficient use of deck space. They can also be actively maneuvered in high-speed patterns to increase lift and generate high towing force [39], similar to airborne wind energy devices [43].

2.3 Academic literature trend and keyword evolution

A comprehensive literature search was conducted across Web of Science, Google Scholar, and Scopus using keyword searches such as "wind-assisted ship (propulsion and technology)", "Flettner rotor", "rotor sail", "wing sail", and "suction sail". The initial search yielded over 400 records, each manuscript underwent a rigorous manual screening process—evaluating titles, abstracts, and full texts for direct relevance to the research scope. Consequently, 212 highly relevant papers were identified for further review. Figure 4 shows the distribution of publication years, highlighting the increasing interest in WAPSs over the past decade, with a surge since 2020.

Figure 5 shows a keyword trend map for visualizing the evolution of research focus. This map captures the temporal development of key topics related to WAPSs. As some terms with identical meanings were expressed differently across publications (e.g., "wind ship" vs. "wind-assisted ship propulsion") and that others were overly broad (e.g., "ship"), the original keyword sets did not always reflect the core content of these studies. Therefore, after carefully reviewing all selected papers, more accurate and representative keywords were reassigned to each paper. Overly generalized or irrelevant terms not pertinent to the present study were excluded from the analysis.

Figure 5 shows that the core topics of WAPS research revolve

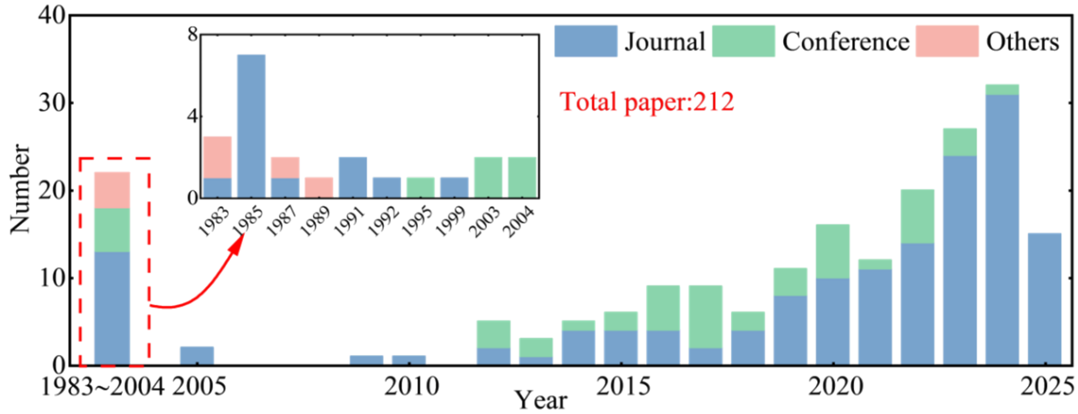

Figure 4 Distribution of publication years (until August 2025).

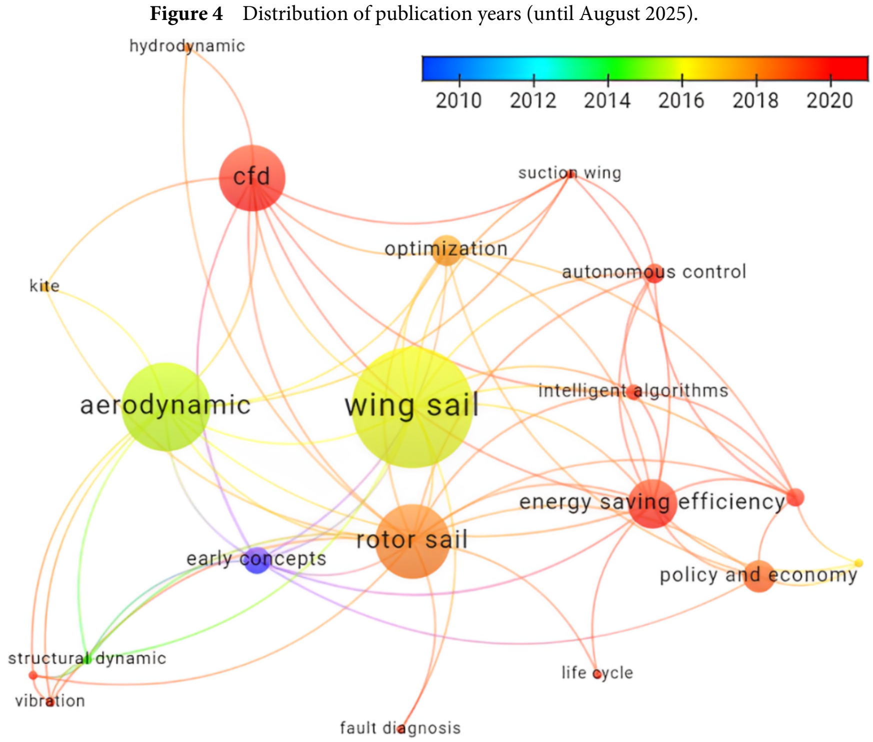

Figure 5 Development trend of literature keywords over time (dot colors represent publication years, dot sizes represent the frequency of occurrence, and connecting lines represent the co-occurrence of keywords in literature).

around "wing sail", "aerodynamic", and "rotor sail", with "rotor sail" gaining increasing popularity since around 2019. Optimization, encompassing both design and operation optimization, has emerged as a key research focus. Although the "suction wing" is currently the most popular WAPS in the industry, it has received considerably less attention in academia; however, interest in this WAPS has been surging recently. This industrial preference for suction wings is mainly driven by their high-lift coefficients, which allow for considerably smaller structural dimensions and lighter weight compared with other WAPSs, thereby minimizing cargo interference. The limited academic attention is due to the proprietary nature of commercial data and the computational complexity associated with simulating active BLC. Research on "kite" remains limited and is declining. Aerodynamics has remained a central aspect of WAPS research, whereas computational fluid dynamics (CFD) has become a popular analytical tool. Compared with aerodynamics, hydrodynamics and structural dynamics have received relatively less research attention. Over the past five years, researchers have expanded beyond performance evaluations and more techno-economic studies have emerged. This reflects the shift in academic research toward the practical implementation of WAPSs in engineering applications. With the rapid advancement of AI technology and the development of unmanned vessels, autonomous control systems and intelligent algorithms are also being integrated into WAPS research.

Table 2 summarizes the reviews published on maritime decarbonization technologies. Among them, three studies [32,44,45] have specifically addressed WAPSs. The first two studies [32,44] mainly reported existing industrial applications and observed impacts, with limited discussion on academic progress and underlying technologies. Wang et al. [45] presented a more comprehensive technical review, covering aerodynamics, optimization designs, and operational control strategies. However, they excluded BLC sails, which are gaining practical relevance. Prior reviews did not analyze research trends, summarize the complete WAPS design procedure or related standards, or consider social and political implications. To address these gaps, this review provides a comprehensive synthesis that integrates academic and industrial perspectives, examines technological advances and challenges, outlines the design procedure and corresponding standards, and assesses the social, environmental, and economic impacts of WAPSs.

2.4 Trends and observations from industrial development

As discussed in Section 1, several factors have accelerated the industrial resurgence of WAPSs. Maritime institutions such as the EMSA [39], LR [40], DNV [41], and ABS [42] have published market reports highlighting the growth and deployment trends of WAPS in the maritime industry. Figure 6 shows the current installations of WAPS based on the classification framework discussed in Section 2.2.

Table 2 List of existing literature reviews of WAPSs

Year	Ref.	Trends		Design			Operation	Impacts			Comments
		Research	Industry	Aerodynamic	Procedure	Standards		Environment	Economy	Society	
2021	[28]		√	√				√			General review on renewable energy for shipping
2021	[32]		√	√			√	√	√		Economic impact and operational considerations of WAPS
2025	[44]		√	√			√	√	√		Industrial applications and potential environmental impact of WAPS
2025	[6]		√	√				√			Overview on current retrofitting maritime decarbonization technologies
2025	[45]		√	√			√	√	√		A detailed technical review of WAPS, with particular emphasis on aerodynamic and operational optimizations, while explicitly excluding BLC sails
2026	[46]		√	√				√			General review on clean energy sources for shipping
This review		√	√	√	√	√	√	√	√	√	A comprehensive techno-economic review on WAPS, including application, principles, design, operation, and impact analysis

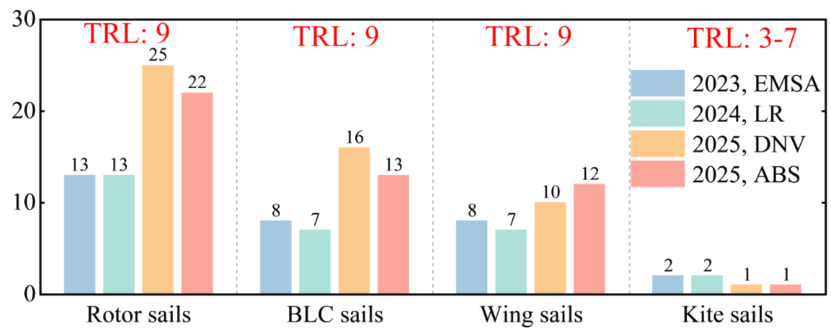

Figure 6 Current industrial WAPS installations based on data obtained from EMSA [39], LR [40], DNV [41], and ABS [42].

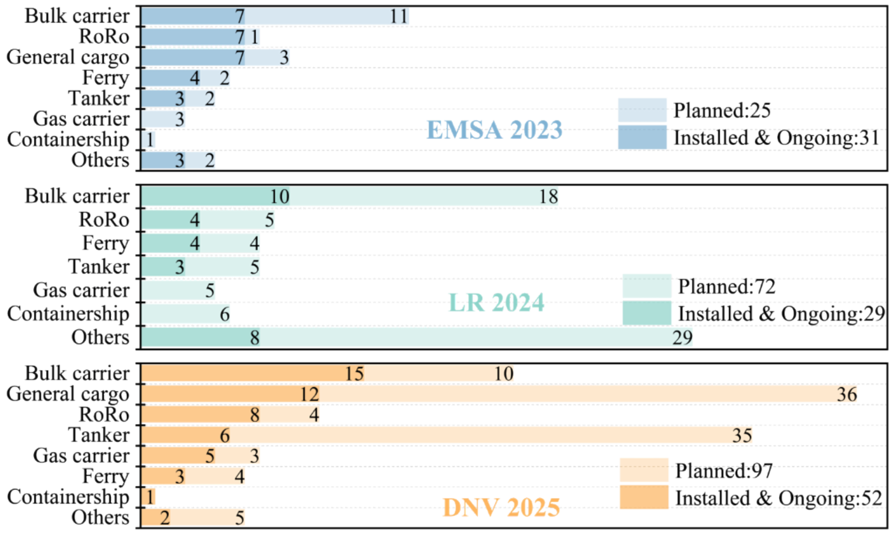

Figure 7 WAPS installations and orders by ship types based on data obtained from EMSA [39], LR [40], DNV [41].

Although slight discrepancies are observed among the three-years datasets collected from various institutions, all sources consistently indicate a steady growth in the adoption of WAPSs. Rotor sails and BLC sails currently dominate the market and exhibit positive growth trajectories. Although BLC sails entered the market relatively late, they have rapidly garnered increased attention across the industry. Wing sails, which once held a substantial market share, have shown stagnation in recent years. Kite sails remain limited in application, with only one or two prototype projects deployed to date. This market shift has also influenced research priorities, redirecting focus from traditional wing sails to rotor and BLC sails (Fig. 5). In terms of technology readiness, rotor sails, BLC sails, and wing sails have reached the technology readiness level (TRL) 9, indicating full commercial maturity. However, kite sails currently remain at TRL levels between 3 and 7 and are under the prototype-level phase. The earliest industrial applications of WAPSs were pioneered in Japan [47]; however, the EU currently leads the market. Previous reviews have reported detailed information on ships equipped with WAPSs [32,44].

Large-scale vessels such as bulk carriers, general cargos, tankers, and RoRo vessels have majorly adopted WAPSs, as shown in Fig. 7. This preference is driven by economic, technical, and operational factors: 1) High fuel consumption: Even a 10%–20% fuel saving (typical WAPS efficiency) has resulted in significant cost reductions. 2) Longer steady ocean routes: Transoceanic routes offer more consistent wind conditions, enhancing WAPS efficiency compared with coastal shipping. 3) Deck space availability: Large vessels can accommodate tall and large WAPSs without obstructing visibility and cargo operations. Additionally, parameters such as speed requirements, noise, and roll stability limit the deployment of WAPSs on small ships.

3 Aerodynamic characteristics of a single WAPS unit

Aerodynamic performance remains the fundamental and critical basis of WAPSs. As each WAPS type operates based on different principles, their aerodynamic characteristics and governing factors differ. Therefore, aerodynamic features must be comprehensively understood for optimizing the geometry of single WAPS units, improving multiunit layout configurations, and ultimately enhancing both economic returns and environmental benefits. Herein, the basic working principles and aerodynamic features of each WAPS type are discussed.

3.1 Working principles of each WAPS type

All WAPSs share a common fundamental objective: harnessing wind energy to generate propulsive thrust via aerodynamic forces (lift and drag) using various methods. When lift and drag are further decomposed and coupled relative to the ship's motion, the component aligned with the ship's forward direction contributes to propulsive thrust and the remaining lateral force acting on the ship induces heel moment.

Rotor sails operate based on the "Magnus effect", as shown in Fig. 8. The Magnus effect refers to the lateral force generated when a rotating object moves through a fluid. This occurs because the object's rotation creates uneven pressure distribution around its surface, generating a force perpendicular to both its spin axis and direction of motion [48]. This effect was experimentally demonstrated by the German physicist, Heinrich Gustav Magnus, in 1852 [49].

BLC sails are based on the principle that effective control of the boundary-layer flow can reduce aerodynamic drag and enhance lift generation. Externally, BLC sails resemble rotor sails: both are vertical columnar structures equipped with endplates. BLC sails are active systems that employ air suction or air jets injection via perforations distributed on the sail surface. The components enabling this functionality include internal active fans, flow suction or jet surface area, and a flap. A typical suction-based BLC sail is illustrated in Fig. 9. As shown in Fig. 9a, when the BLC sail is inactive under unfavorable wind conditions, it operates similar to a

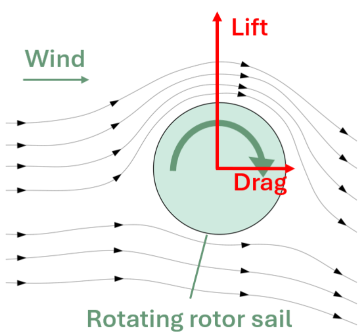

Figure 8 Working principal of the rotor sail: Magnus effect.

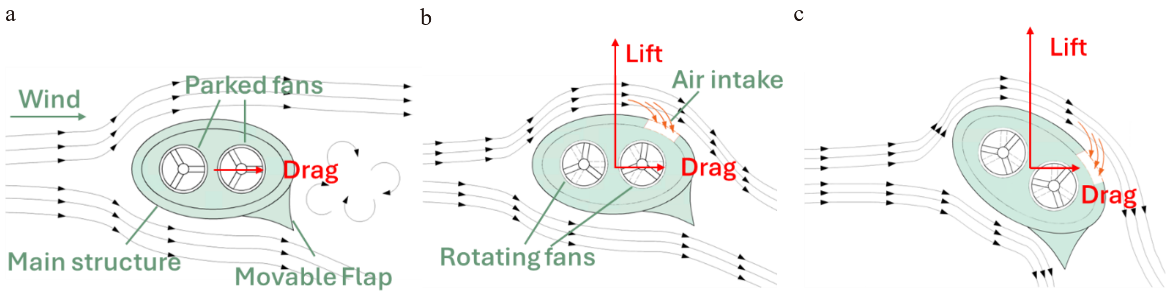

Figure 9 Working principle of BLC sails: Suction BLC is taken as an example, with boundary-layer control and AOA adjustment shown. (a) No BLC status. (b) BLC by air intake. (c) BLC and AOA adjustment.

conventional wing profile. The lift coefficient increases with profile thickness and angle of attack (AOA) until the flow separation occurs at the stall point. Beyond this, flow detachment leads to reduced lift and considerably increased drag, resulting in poor aerodynamic performance.

Upon activating the boundary-layer suction via internal fans, the sail ensures the air flow remains adhered to the sail surface to generate high lift. By adjusting the AOA (Fig. 9c), BLC sails can achieve a maximum lift coefficient C_L of 8.3 (a result that has been independently validated by DNV) [50] while maintaining smaller sizes and lower weights. In addition to air suction [51–55], other BLC strategies such as co-flow jet [56,57] and circulation control [57] are employed. Fundamentally, all BLC approaches aim to manipulate the local boundary-layer flow to enlarge the pressure differential between the windward and leeward faces of the sail, thereby achieving higher lift.

Wing sails generate aerodynamic forces by altering the airflow around them and creating a pressure differential between the windward and leeward surfaces (Fig. 10). Lift and drag forces are generated via the combined influence of wing shape and its AOA relative to the airflow [58]. In aviation, airfoils are typically asymmetric, with a longer and more curved upper surface to improve lift. However, such asymmetric designs are not well suited for maritime WAPSs. Due to constantly changing wind directions and vessel headings, wing sails often adopt symmetric airfoil profiles to ensure consistent performance (Fig. 11). Due to the limited thrust generated by single symmetric wing sails, existing studies have mainly focused on crescent-shaped wing sails (Fig. 11a) and multielement wing sails (Fig. 11b). Crescent-shaped wing sails or arc wing sails have a symmetric sectional profile with a certain degree of curvature. Multielement wing sails combine multiple individual wings or comprise a main wing integrated with flaps, noses, or slats. Most wing sails maintain a consistent cross-sectional size along the vertical axis, whereas others taper with a reduced cross-section toward the top.

Kite sails generate lift and drag by harnessing stronger winds at high altitudes, typically between 150 m and 400 m above sea level. They operate at elevation angles between 10° and 35° [42] relative to the horizon (Fig. 12a). Kite sails function as flexible airborne traction systems, and its key components are shown in Fig. 12b. Current kite sail concepts mainly employ foil kites, which are double-layered structures composed of multiple canopy cells extending from the leading edge to the trailing edge. These cells form a cross section that exhibits superior aerodynamic efficiency with compared with single-surface alternatives [43,82] and can be manufactured at large surface areas [43]. This makes kite sails more suitable for WAPSs. The kite is fabricated from high-performance textile materials and sectioned as an airfoil, as shown in Fig. 12c. It is connected to the vessel via steering tethers to a control pod, which houses the autopilot system responsible for steering the kite and maintaining optimal flight trajectories. By adjusting the kite's orientation relative to the apparent wind, the control pod guides it along dynamic flight paths—typically a figure-eight trajectory (Fig. 12a)—to maximize lift and drag generation. The resulting aerodynamic forces are transmitted to the ship through the towing tethers, providing forward propulsion via the kite's towing force. Kite sails are effective when operating in reaching courses or side downwind conditions, where the AOA maximizes lift, rather than running courses or full tailwind conditions [42,83].

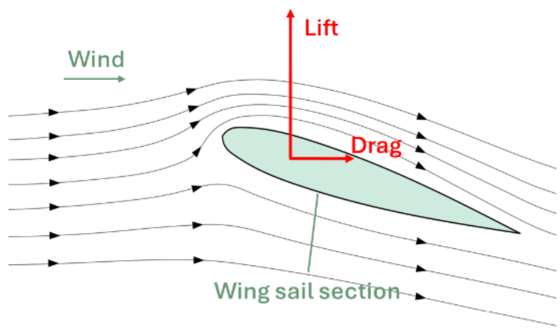

Figure 10 Working principle of wing sails: Sectional shape and AOA adjustment.

3.2 Influential factors on WAPS unit aerodynamics

An analysis of the working principles of WAPSs revealed that their aerodynamic performance is mainly governed by three groups of

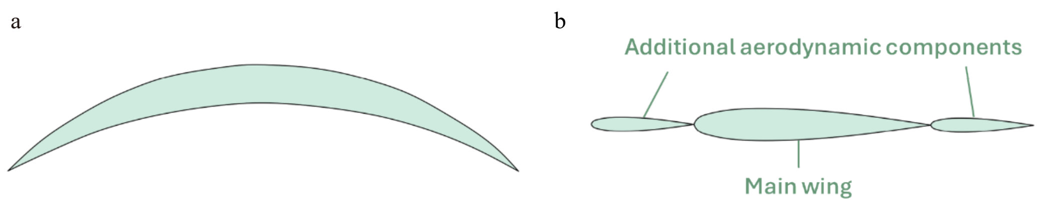

Figure 11 Different cross-sectional shapes of wing sails. (a) Crescent-shaped wing sails [59–69]. (b) Multielement wing sails [70–81].

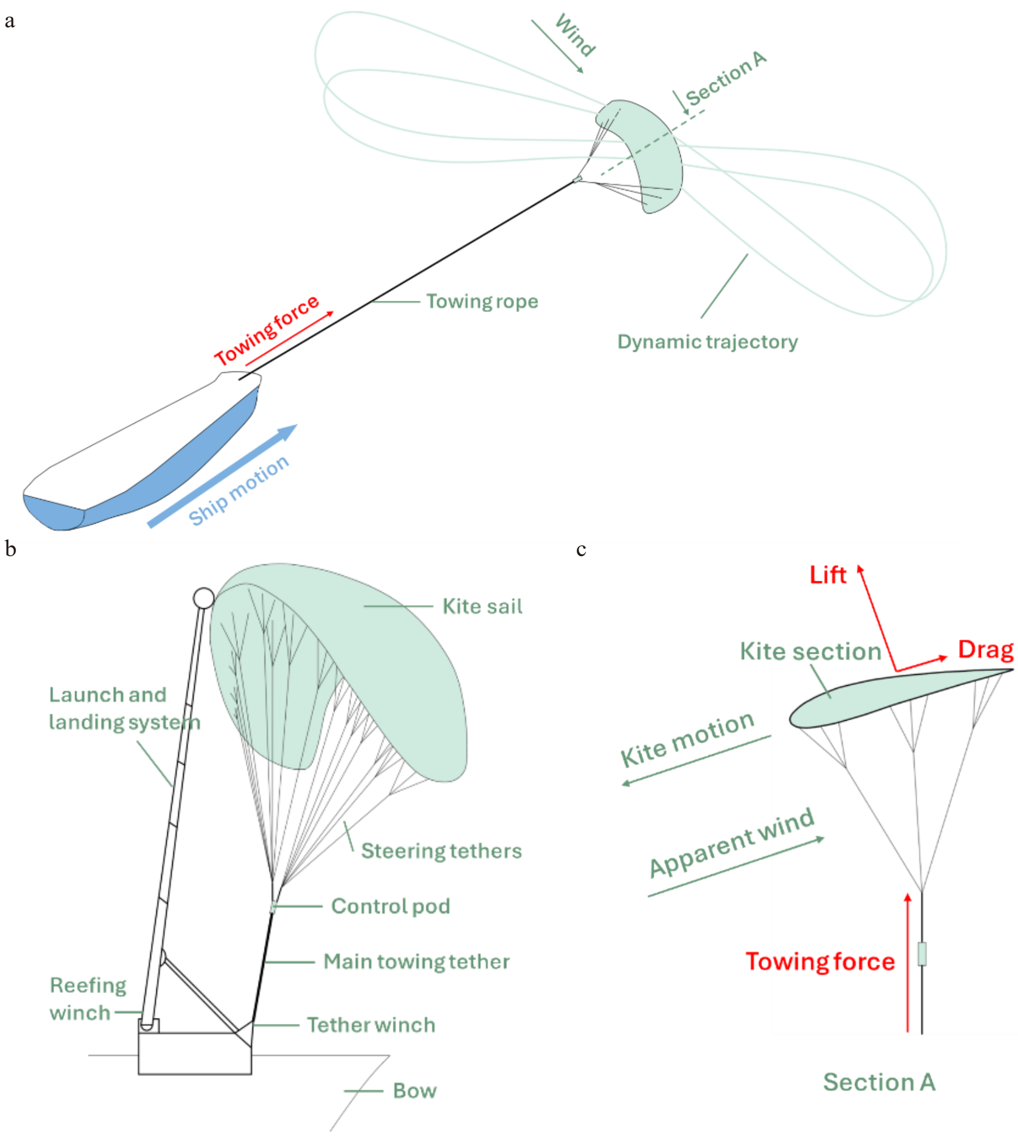

Figure 12 Illustrations of the working principle for kite sails. (a) Overview, dynamic trajectory, and the installation on ships. (b) Main system components, redrawn from Ref. [42]. (c) Airfoil cross section and associated aerodynamics.

factors: (i) wind conditions, (ii) WAPS geometry, and (iii) WAPS control strategies.

3.2.1 *Qualitative comparison under varying wind conditions*

In maritime navigation, wind conditions are typically categorized into true wind and apparent wind. True wind refers to the actual wind speed and direction relative to the Earth, independent of the vessel's movement. In contrast, apparent wind is the wind experienced by a moving ship, obtained from the vector combination of true wind velocity and ship velocity.

Existing experimental and numerical studies have investigated optimal true wind conditions for the effective operation of different types of WAPSs. The resulting polar diagrams in Fig. 13 illustrate the aerodynamic performance across different true wind angles and speeds. Although the source data for these polar diagrams were obtained from different publications—featuring varying vessel speeds, true wind speeds, and radial metrics (e.g., power reduction, power output, and fuel savings)—the comparison remains qualitatively valuable. These diagrams reveal the operational true wind ranges and performance suitability for each WAPS type. They typically show a 0°–180° range, assuming symmetry at the longitudinal axis. The red arrow in the polar plot indicates ship heading, with varying ship speeds; the colored lines represent propulsion efficiency under different true wind speeds; and the polar angle represents the wind flow direction, with 180° corresponding to a pure headwind condition.

All WAPS types exhibit optimal performance under tail-side true wind angles of approximately 30°–90°. Under these conditions, the apparent wind—the vector sum of the true wind and the vessel's forward velocity—tends to approach crosswind orientation relative to the vessel, which best match the operating principles of WAPS. Among them, BLC sails and wing sails demonstrate the broadest effective range of true wind angles because they can actively adjust AOA; thus, they exhibit some operational capability even under headwind conditions. Rotor sails also perform strongly under such conditions; however, their performance declines under side headwind conditions. Kite sails exhibit the narrowest operational envelope because their tethering system restricts their ability to

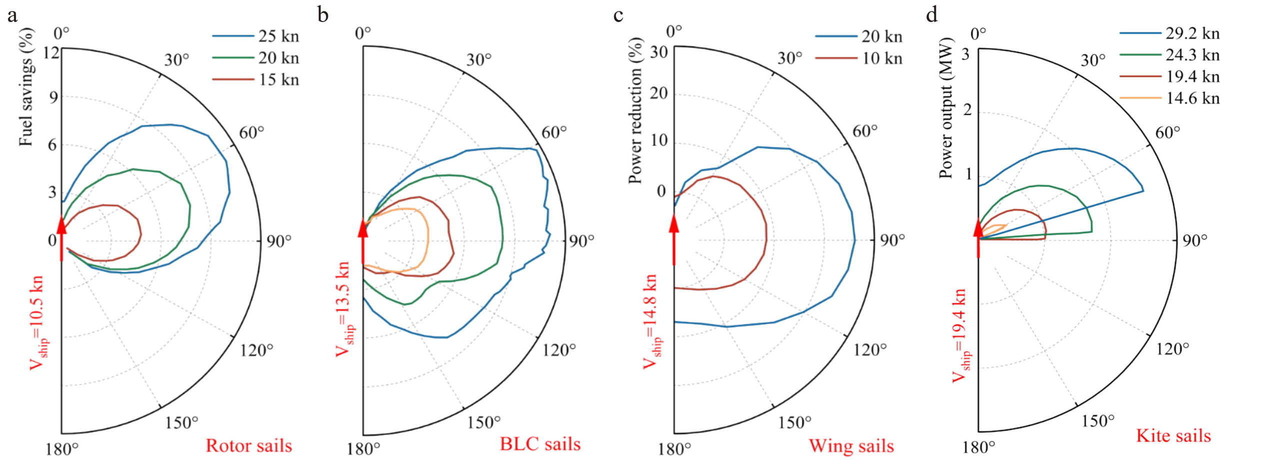

Figure 13 Polar diagrams of each WAPS type as a function of true wind angle, assuming a ship course of 0° (indicated by the red arrow). (a) Rotor sails [84]. (b) BLC sails [51]. The exact wind speeds and radial metrics of BLC sails are not available in the cited study due to commercial confidentiality. (c) Wing sails [63]. (d) Kite sails [83].

generate propulsion under headwind conditions.

With respect to wind speed, a general trend can be observed that higher true wind speeds typically result in greater propulsion efficiency for WAPSs. This highlights a potential operational strategy: by adjusting the ship's velocity to optimize the apparent wind angle, more favorable wind conditions for the operation of WAPSs can be created for further enhancing their performance.

3.2.2 Effects of WAPS geometry on aerodynamics

Geometric design considerably influences the propulsion efficiency of WAPS units. As each WAPS type have distinct working principles, different geometric parameters play critical roles in shaping their aerodynamic performance.

Rotor sails typically contain a fixed rotating cylinder with a circular cross section. However, several geometric parameters significantly affect their aerodynamic performance. The first parameter is the aspect ratio [85,86], which the ratio of rotor height to diameter. Higher aspect ratios increase lift-to-drag ratios, indicating enhanced aerodynamic efficiency. Another parameter is the endplate size, which suppresses adverse three-dimensional flow effects and tip vortices at the rotor ends [87]. Introducing rough surfaces to rotor sails can delay boundary-layer separation, reduce the low-pressure wake region behind the rotor, and ultimately decrease aerodynamic drag [48].

The aerodynamic performance of BLC sails is influenced by geometric factors such as the cross-sectional profile, internal BLC components, endplates, and additional aerodynamic devices. The choice of cross-sectional profile is largely driven by aerodynamic efficiency and the need to accommodate internal BLC components, leading to the widespread adoption of near-circular geometries and influencing optimal AOA. Common profile geometries include circular, elliptical, and egg-shaped sections [51,53–55,88–91], as well as conventional airfoil profiles [56,57]. These internal BLC components determine the specific flow-control strategies implemented such as air suction [51–55], co-flow jets [56,57], and circulation control [57]. The achievable aerodynamic performance depends on the size, placement, and momentum intensity of the suction or jet slots integrated into the system. Endplates are also recommended for BLC sails to mitigate the formation of end vortices [53], and auxiliary aerodynamic components such as flaps are often integrated. These flaps can increase camber and effective AOA, thereby increasing net circulation and ultimately enhancing lift generation [54,90]. They also help delay stall and stabilize performance under higher AOAs [57,90]. Flap designs have evolved from simple fixed plates [55,88] to more advanced movable triangular configurations [53,54,91].

The performance of wing sails are primarily influenced by their cross-sectional geometry and additional aerodynamic components. Most studies have focused on crescent-shaped wing sails [59,63–65] and multielement wing sail configurations [71,72,74,75], which offer higher potential of performance enhancement and design innovation compared with conventional airfoils. These configurations involve detailed parametric variations, including relative element lengths, angular offsets, and inter-element spacing. The addition of endplates can provide modest improvements in aerodynamic performance [63–65]. Furthermore, auxiliary aerodynamic components such as flaps, leading-edge noses, and slats are often incorporated [74,75,81,92] into wing sail systems, drawing inspiration from aeronautical engineering.

Kite sails can adopt various airfoil cross sections [43,82], and their inflatable structures provide large surface areas suitable for propulsion applications [43]. These sails may employ one, two, or multiple main tethers, and this configuration directly affects aerodynamic drag [93–96]. The associated drag penalty becomes more significant with increasing tether length, particularly during high-altitude operations. The overall system efficiency can be improved by employing faired or aerodynamically shaped tethers [97].

3.2.3 Effects of WAPS control on aerodynamics

Beyond geometric design, control strategies play a crucial role in determining the actual aerodynamic performance of WAPSs under real operating conditions.

The primary control mechanism for rotor sails is rotational speed adjustment, which modulates the strength of the Magnus effect. By varying the spin ratio [85,86,98–101], operators can modulate the lift force generated perpendicular to the wind direction. Higher spin ratios produce greater lift while increasing auxiliary power consumption and heel moments. Thus, the control objective is to identify an optimal spin ratio that maximizes net propulsion efficiency while maintaining acceptable heel angles and minimizing auxiliary power requirements under varying wind conditions.

For BLC sails, three coordinated factors are used to achieve control: BLC intensity, AOA adjustment, and trailing edge flap adjustment. BLC intensity is determined by the power supplied to internal fans, which controls the momentum flux of air removed from (or injected into) the boundary layer through surface perforations. An optimal BLC intensity exists for each operating condition [51–57]: insufficient momentum injection fails to prevent flow separation, whereas excessive injection results in diminishing aerodynamic returns relative to power input. AOA adjustment enables the sail to rotate about its vertical axis to adapt to varying apparent wind conditions [56,91]. The optimal AOA is coupled with BLC intensity: higher BLC intensity extends the effective operating envelope to larger AOA. Trailing edge flaps [53,54,57,88,90,91] modify the effective camber, delay stall via improved pressure recovery on the leeward surface, and provide an additional degree of freedom for lift enhancement.

For wing sails, control primarily focuses on AOA adjustment [60,63–65,75,81] to align the sail optimally with apparent wind and maximize the lift-to-drag ratio. In the absence of active BLC, wings sails are more susceptible to flow separation at high AOAs. Additionally, many wing sail designs incorporate movable aerodynamic components such as flaps, slats, and leading-edge noses [63–65,74,75,81,92], which can be adjusted to optimize the pressure distribution and increase maximum achievable lift under various wind conditions.

The flight trajectory considerably influences the aerodynamic performance of kite sails. Flying the kite along paths perpendicular to the apparent wind such as figure-eight [42] or circular patterns [83] can considerably increase apparent wind speeds, thereby enhancing the generated aerodynamic forces. Trajectory control also comprises active AOA adjustment [102,103] and modulation of turning rate [104], which are also critical for maximizing propulsion efficiency.

The geometric and control-related influential factors of each WAPS type and the corresponding references are summarized in Table 3. Rotor and wing sails involve relatively fewer design and operational factors, whereas BLC sails are more complex due to their internal flow-control components. Kite sails pose challenges primarily in controlling their flight trajectories.

4 Design of WAPSs

To design reliable WAPSs, comprehensive guidelines addressing key considerations and elements are essential. These guidelines include the definition of operational conditions, the optimization of design variables, and the selection of appropriate evaluation methods. This section outlines general principles and considerations relevant to the design of WAPSs.

4.1 General design considerations and procedure

The fundamental design objectives of WAPSs include safety, efficiency, and cost-effectiveness. In essence, the objective is to develop efficient WAPSs that enable the host vessel to operate safely while minimizing lifecycle costs. Figure 14 shows the flowchart of the WAPS design process comprising four main stages.

The concept design phase focuses on defining design inputs, including the ship specifications (visibility constraints, available deck space, and other parameters); marine environmental conditions; design constraints, and overall budget.

The preliminary design stage determines a set of fundamental options based on prior experience and design inputs, including the WAPS type, unit dimensions, and material selection. Low-fidelity tools such as theoretical models and empirical databases are employed to perform life cycle assessment (LCA) and life cycle cost (LCC), along with a basic safety evaluation under anticipated load conditions. The first two stages are also often referred to as front-end engineering design.

The detailed design stage includes the development of specific layout configurations (excluding kite sails), detailed component design, and comprehensive safety checks against various limit states in accordance with applicable standards. This stage is typically executed under the engineering, procurement, and construction mode. At this stage, high-fidelity tools such as CFD, finite element method (FEM) simulations, and wind tunnel experiments are used to perform the in-depth analyses of operational safety and propulsion performance.

An independent third-party verification is conducted by a classification society prior to obtaining formal approval.

The remainder of this section outlines technical design considerations, and the economic aspects are presented in Section 6.1.

4.2 Overview of WAPS components

Multiple subsystems are required for the efficient operation of WAPSs; these subsystems can be categorized into five groups: WAPS units, electrical and machinery systems, foundation and stowage systems, sensors and monitoring systems, and global control system. Using rotor sails as an example, the WAPS components are shown in Fig. 15. Among these subsystems, the WAPS units are closely linked to various objectives and variables in structural design; these will be discussed in detail in Section 4.3. The global control system, which governs integration with ship operations, will be discussed in Section 5.

This section focuses on the remaining subsystems.

Table 3 Working principles of WAPS and their influential factors

Type	Rotor sails	BLC sails	Wing sails	Kite sails
Working principles	Magnus effect	Active boundary-layer flow control	Sectional shape and AOA adjustment	Sectional shape and dynamic trajectory
Geometry	Aspect ratio [85,86], endplate [48,85–87], and surface roughness [48,105–109]	Cross-section [51,53–57,88–91], internal BLC components [51–57], endplate [53], and aerodynamic components [53,54,57,88,90,91]	Cross-section [59,63–65,71,72,74,75] and aerodynamic components [63–65,74,75,81,92]	Kite section and area [43,82,83] and tether [93–97]
Control	Spin ratio [85,86,98–101]	BLC intensity [51–57], AOA [56,91], and aerodynamic components control [53,54,57,88,90,91]	AOA [60,63–65,75,81] and aerodynamic components control [63–65,74,75,81,92]	Flight trajectory [43,83,96,102–104]

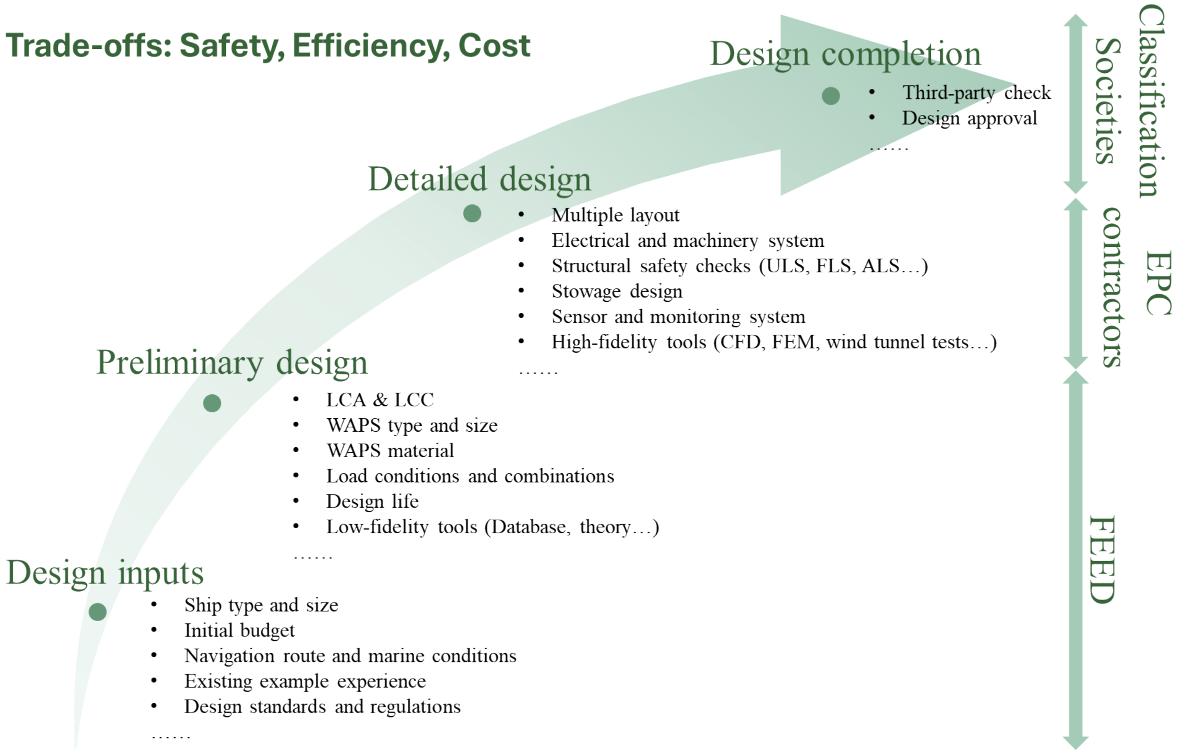

Figure 14 Flowchart of the WAPS design process with key elements.

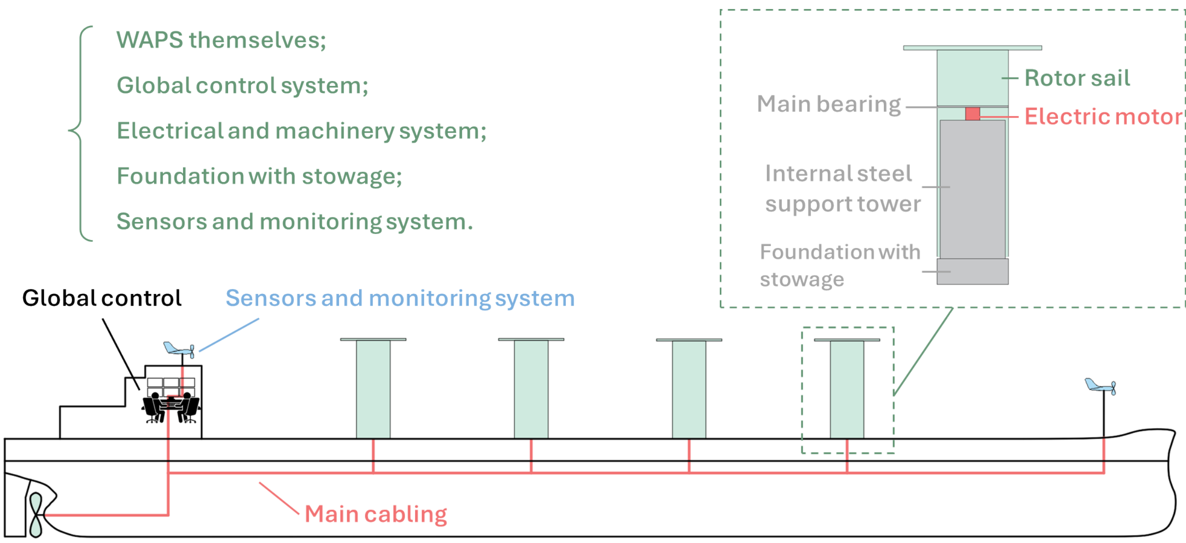

Figure 15 WAPS components installed on a vessel equipped with rotor sails.

4.2.1 Electrical and machinery systems

Each WAPS type requires auxiliary power to activate its propulsion functions. Rotor sails require power to maintain continuous rotation. BLC sails require power for active boundary-layer suction or blowing, as well as for AOA adjustments. Wing sails rely on actuators to control AOA and adjust aerodynamic components such as flaps. Kite sails require power for steering the tether lines and executing dynamic flight trajectories. To support these operations, integrated electrical and mechanical systems are essential, including motors, actuators, sensors, and control units. Only a few studies have focused on these detailed component designs and optimization [110]; however, classification societies have published some relevant technical requirements [111–116].

4.2.2 Sensors and monitoring systems

As discussed in Section 3.2.3, the active control of WAPSs under varying wind and marine conditions is essential for optimizing aerodynamic performance, which subsequently maximizes overall propulsion efficiency. Therefore, integrating environmental sensors [117,118] that can detect and predict surrounding conditions is necessary. For rotor sails, BLC sails, and wing sails, onboard sensors are generally sufficient to meet this requirement. Kite sails, which operate at high altitudes, benefit more from sensor installations on the airborne control pod for accurately capturing operational wind conditions. In addition, structural health monitoring systems [119] are valuable for maintaining WAPS integrity and ensuring reliability against the limit states discussed earlier.

4.2.3 Stowage

Efficient and reliable stowage designs are essential for the practical implementation of WAPSs. Their functions extend beyond reducing aerodynamic drag under unfavorable wind conditions; these designs are also critical for ensuring navigational safety during port maneuvers, clearance under height-restricted structures, and safeguarding the system against damage under harsh marine environments.

As previously discussed, kite sails can be stowed easily due to their flexible and soft textile design. In contrast, rotor sails, BLC sails, and wing sails require dedicated mechanical systems for stowage. Three mainstream stowage designs are currently employed (Fig. 16): tiltable, retractable, and liftable configurations.

Tiltable stowage is widely adopted, as shown in Fig. 16a. In this configuration, the WAPS base is partially fixed to the deck via a hinge or pivot mechanism that enables the structure to tilt. This approach is broadly applicable because it maintains the structural integrity of WAPSs. However, it requires dedicated deck space, introduces additional weight, and is highly cost-intensive, considerably increasing the overall expenses. Retractable stowage [60,63–65,81], as shown in Fig. 16b, is primarily used for wing sails. The sail is segmented into multiple sections that can be retracted along an internal guiding beam. While this configuration offers compact stowage, it compromises the structural integrity of WAPSs and is therefore unsuitable for rotor or BLC sails containing complex internal components. Liftable stowage, as shown in Fig. 16c, is less developed and less commonly applied. In this configuration, the WAPS unit is mounted on a vertically movable base; this allows the entire WAPS to drop below the deck level. This configuration requires dedicated below-deck space. As most current WAPS installations are retrofits on existing vessels, rearranging internal ship space is generally infeasible. However, liftable stowage may present a viable option for newly built ships.

4.3 Objectives and variables of structural design

WAPS design involves numerous technical objectives and variables. These design parameters must be combined to meet the structural and operational constraints. The key design variables relevant to structural design are discussed herein.

4.3.1 Geometry, size, and material

The geometric parameters influencing each WAPS type were discussed in Section 3.2.2. After selecting a WAPS type, its geometric configuration is defined within a design space that is informed by prior applications and developer experience. The overall dimensions are primarily determined by the vessel specifications, particularly available deck space and required thrust contribution.

Steel remains the primary material for WAPS design; however, lightweight and high-strength alternatives such as carbon fiber composites are also increasingly adopted [39]. In general, selected materials must comply with standard shipbuilding requirements, particularly in terms of strength, fatigue resistance, and corrosion protection. Several classification societies have already established guidelines to support the material selection [111–113].

4.3.2 Layout of multiple WAPS units

Multiple WAPS units, except for kite sails, are typically installed to ensure sufficient and consistent thrust generation, rather than relying on a single unit. However, aerodynamic interactions among multiple WAPS are unavoidable due to limited deck space. Designing optimal layouts therefore remains a critical engineering challenge.

Taking rotor sails as an example, two typical multiple-unit layouts are illustrated in Fig. 17: single-row and multirow configurations. Layout selection depends primarily on the available deck space and the prevailing apparent wind conditions along intended navigation routes. Numerous studies have investigated the aerodynamic performance of various layout configurations for rotor sails [85,98,99,120] and wing sails [60–62,70,78,81,92,121]. These studies have shown that wake flow disturbances from upstream units degrade the aerodynamic performance of downstream WAPS units. Consequently, system-level control strategies have been proposed to mitigate these adverse interaction effects and enhance the overall propulsion efficiency. One approach involves operating certain upstream WAPS units to improve the overall system performance [60,61,121,122]. Another strategy involves reutilizing the wake energy by optimizing the relative positioning of WAPS units [123].

4.3.3 Performance uncertainty of WAPS

WAPSs share similarities with floating offshore wind turbines; their aerodynamic performance is strongly influenced by variable real-sea conditions and complex platform motion [124]. For WAPS, except for kite sails, the primary sources of performance uncertainty include: (1) real marine wind profile, (2) aerodynamic disturbances caused by the hull and superstructure, and (3) ship motions,

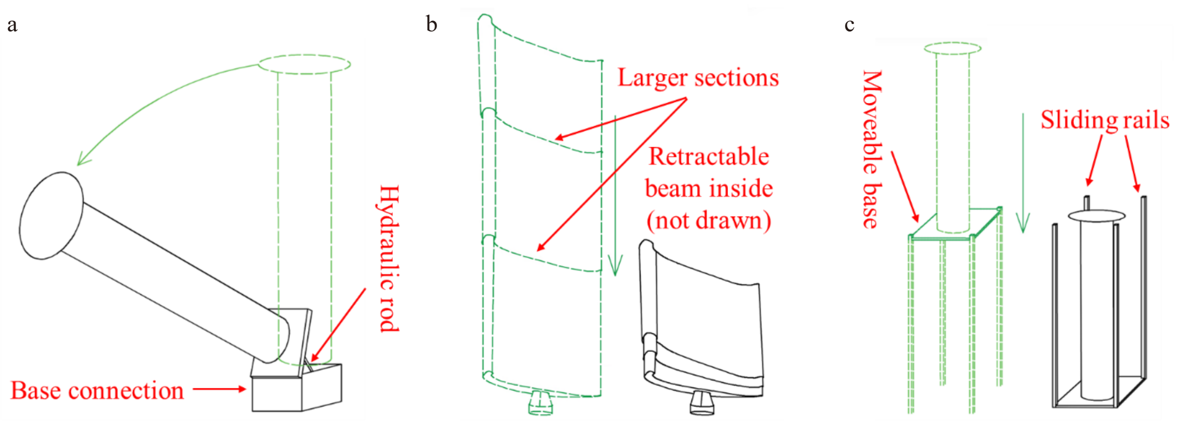

Figure 16 Current mainstream stowage configurations for WAPSs. (a) Tiltable stowage. (b) Retractable stowage. (c) Liftable stowage.

https://doi.org/10.26599/OCEAN.2026.9470019

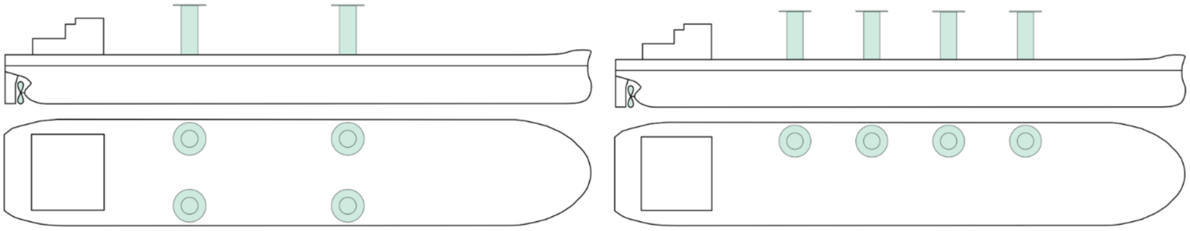

Figure 17 Typical multiunit WAPS layouts: 2 × 2 and 1 × 4 rotor sail configurations.

particularly roll. These factors are critical but are often overlooked in existing design-oriented research.

Due to the effects of the marine atmospheric boundary layer [125], wind speed near the sea surface exhibits a vertical shear profile. This gradient wind field reduces the ideal aerodynamic efficiency of WAPSs compared with that observed under uniform wind conditions [66,122,126–131]. Wind shear also increases structural risks by inducing higher bending moments at the base of WAPSs [101].

Most existing studies have focused solely on WAPS performance without accounting for flow disturbances introduced by the hull and superstructures. However, these structures combined with the gradient wind profile, particularly when located upwind of the WAPS, can considerably reduce propulsion efficiency compared to idealized calculations [53,78,127,132].

Operational vessels are subject to roll, which can be further amplified by the heel moments generated by WAPSs. This coupling between ship motion and aerodynamic loading, in turn, affects the aerodynamic performance of WAPSs. Existing studies have analyzed the uncoupled effects of ship roll on WAPS performance [66,131,133] and the impact of WAPS on amplifying roll [68,120,133,134]. However, fully coupled aero-hydrodynamic analyses remain scarce. To mitigate the adverse effects of ship motions, a promising solution is to equip WAPSs with attitude stabilization systems that can maintain optimal aerodynamic orientation [135–137].

Compared with deck-mounted systems, kite sails are less affected by disturbances induced by hull and wind shear as they operate at higher altitudes. However, time-varying wind conditions still pose challenges in maintaining optimal propulsion performance [96]. Additionally, the use of flexible tether ropes adds further complexity to the coupled aero-hydrodynamic dynamics of this system [83].

4.4 Safety constraints

Clarifying the design loads and corresponding limit states is essential for ensuring the structural safety of WAPSs. Design loads are generally categorized into regular service loads, extreme loads, fatigue loads, accidental loads, and other loads. Their associated contributors, operational conditions, and limit states are summarized in Table 4.

The ultimate limit state (ULS) corresponds to the maximum load-carrying capacity of the WAPSs. ULS-based design requires structural assessment under both regular service and extreme load conditions [138]. Under regular service loads, structural strength must be evaluated considering wind loads and inertia loads induced by ship motions. Under extreme loads, more severe wind conditions and intensified ship motions must be considered. Environmental loads such as green water impact, spray loads during harsh sea states, snow and ice accumulation [139], and thermal loads due to low temperatures—particularly relevant for kite sails operating at high altitudes—should also be considered. The fatigue limit state (FLS) relates to structural failure resulting from cyclic loading [140], with particular concern for high-frequency vibrations induced by wind loads [63–65,100]. These effects are crucial for the bottom connections of the rotor, BLC, wing sails, and tension fluctuations in kite sail cables. The accidental limit state (ALS) addresses structural survivability under damaged or abnormal conditions such as ship collisions [141] or onboard fires [142], ensuring the integrity of WAPS under rare but severe scenarios.

By verifying the performance of WAPSs under the aforementioned limit states, their design service life can be estimated. This service life should exceed the remaining life of the host vessel, but not excessively, to balance safety requirements with cost efficiency. Although specific regulations for the reliability index of WAPSs have not yet been established, insights can be drawn from existing ship structural standards. For example, the reliability index of primary ship structures typically ranges from 2.79 to 5.38 [143], whereas those of local structural components often begin at ~3.5 but may decrease to ~2.0 when serviceability limits are

Table 4 Categorization of design loads for WAPSs [111]

Design loads	Possible load contributors	Description
Regular service loads	Wind loads and ship motion inertia	WAPSs in operation at the upper limit of their operational envelope, i.e., delivering full aerodynamic capacity; used for ULS strength assessments
Extreme loads	Wind loads, ship motion inertia, snow and ice, green sea and spray water, and thermal loads	WAPSs in stand-by or out of operation; used for ULS strength assessments
Fatigue loads	Wind loads, ship motion inertia, and high-frequency loads	WAPSs in operation; cyclic loads are used for FLS strength assessments
Accidental loads	Collisions and fires	WAPSs under any operating conditions including transition; unforeseen and potentially damaging loads for ALS strength assessments
Other loads		As applicable on a case-by-case basis

Note: Definitions of operational conditions: In operation: WAPSs are deployed and generate auxiliary propulsion power. In stand-by WAPSs are not generating auxiliary propulsion power, i.e., de-powered or parked during extreme weather conditions. Out of operation: WAPSs are not generating auxiliary propulsion power, i.e., in harbor mode or when retracted or tilted and secured. Transition: WAPSs during tilting or retraction sequence from unlocked stand-by to unlocked tilted or retracted.

considered [144]. Accordingly, an initial reliability index of 2.5–3.5 could be considered appropriate for WAPS safety design.

Rotor sails, BLC sails, and wing sails can simply be considered cantilever columns subjected to lateral dynamic loads. In contrast, the primary structural challenge for kite sails lies in the integrity and reliability of their cable systems that are subjected to complex tensile loads. Many existing studies have overlooked these critical structural concerns, and only a small number of studies have analyzed the structural vibrations of rotor and wing sails [63–65,100] and proposed solutions to address these issues [100,110,145,146].

Moreover, existing studies analyzed WAPSs using uncoupled fluid–structure interaction methods [100] or simplified approaches such as preloadings [146]; these methods may underestimate the effects of high-frequency aerodynamic excitations on the performance of WAPSs. With recent advancements in aerodynamics, high-fidelity coupled aeroelastic analyses have become feasible [147–149]. By extending these techniques to WAPSs, valuable insights into structural safety can be obtained under realistic operational conditions.

4.5 Numerical modeling tools

Design tools play a crucial role in the WAPS design process. Employing appropriate modeling methods at each design stage can help achieve design objectives with reduced resource consumption.

Low-fidelity tools primarily include theoretical formulas and data-driven empirical methods. Theoretical approaches comprise aerodynamic drag and lift equations, beam theory for structural dynamics, and the DNV-RU-SHIP inertia calculations [150]. Empirical methods are derived from datasets generated via previous high-fidelity simulations or wind tunnel experiments [122].

Mid-fidelity tools refer to simulation approaches based on simplified assumptions such as OpenFAST [130], panel method [55,90], and in-house codes [151]. Low- and mid-fidelity tools are normally employed during the preliminary design stage to rapidly evaluate the baseline performance of WAPS.

High-fidelity methods, such as CFD [63,129] and FEM [100], are widely employed for the in-depth simulation of the aerodynamic and structural behavior of WAPSs under complex marine conditions. These tools are also effective for analyzing aerodynamic interactions among multiple WAPS units [99] and their coupling with ship hydrodynamic motions [66].

Although less ubiquitous and costlier compared with other numerical methods, wind tunnel testing [85,120,152] remains an essential standard approach for validating numerical predictions. In addition, the physical scaled modeling of WAPSs with coupled aerodynamic and hydrodynamic effects is intrinsically challenging because it must reconcile conflicting requirements of Froude similarity (that governs wave-induced hydrodynamics) and Reynolds similarity (that is critical for capturing wind-induced aerodynamic loads) [153]. However, some insights can be drawn from the experimental research on current floating wind turbine using real-time hybrid testing.

4.6 Design standards and guidelines

To standardize and safeguard WAPS development, various classification institutions have issued design standards and guidelines; these are summarized in Table 5. These documents provide recommendations on structural loading, WAPS configuration, material selection, strength assessment, and crew safety. In addition to standards directly related to WAPS design, general ship regulations such as COLREG, the anti-collision rules, must still be followed.

Despite these advancements, existing standards remain general due to limited operational experience. Many documents do not contain WAPS-specific provisions and omits considerations related to kite sails. Detailed and specific standards are required to address constraints, technical design details, operational notices, and safety concerns for WAPSs and addressing additional issues introduced by integrating WAPSs into vessels.

5 Operational challenges of WAPS-integrated ships

The integration of WAPSs introduces a distinct shift in ship operations. Vessels equipped with WAPSs are encouraged to exploit wind conditions rather than consistently operating against natural forces. Although this shift offers potential benefits, such as significant reductions in fossil fuel consumption, minimized greenhouse gas emissions, and improved regulatory compliance, it simultaneously introduces new issues, which are discussed in this section.

5.1 WAPS-oriented weather routing

Global weather routing [155–158] is a decarbonization measure, which typically achieves fuel reductions of ~10% [6]. This method may employ a longer route to avoid strong headwinds and high seas, ultimately saving fuel and arriving on time.

WAPS-oriented weather routing operates at a macro level and involves strategic port-to-port planning, as shown in Fig. 18. This approach seeks to determine the optimal global trajectory—specifically defined as the route that minimizes fuel consumption

Table 5 Summary of relevant standards and regulations for WAPS design

Institution	Edition	Title
Bureau Veritas (BV), France	March 2025	NR206 Wind Propulsion Systems [112]
Lloyd's Register (LR), England	January 2024	LR-GN-044 Guidance Notes on Wind-Assisted Propulsion Systems [154]
Korea Register (KR), Korea	2025	Guidance for Prevention System of Pollution from Ships, Chapter 5, Wind-Assisted Propulsion System [116]
Det Norske Veritas (DNV), Norway	December 2023	DNV-ST-0511 Wind-Assisted Propulsion Systems [111]
Nippon Kaiji Kyokai (ClassNK), Japan	April 2023	Guidelines for Wind-Assisted Propulsion Systems for Ships (Edition 2.0) [114]
China Classification Society (CCS), China	February 2023	Guidelines for Survey of Marine Wind-Rotor-Assisted Propulsion System [115]
American Bureau of Shipping (ABS), The US	July 2022	Requirements for Wind-Assisted Propulsion System Installation [113]

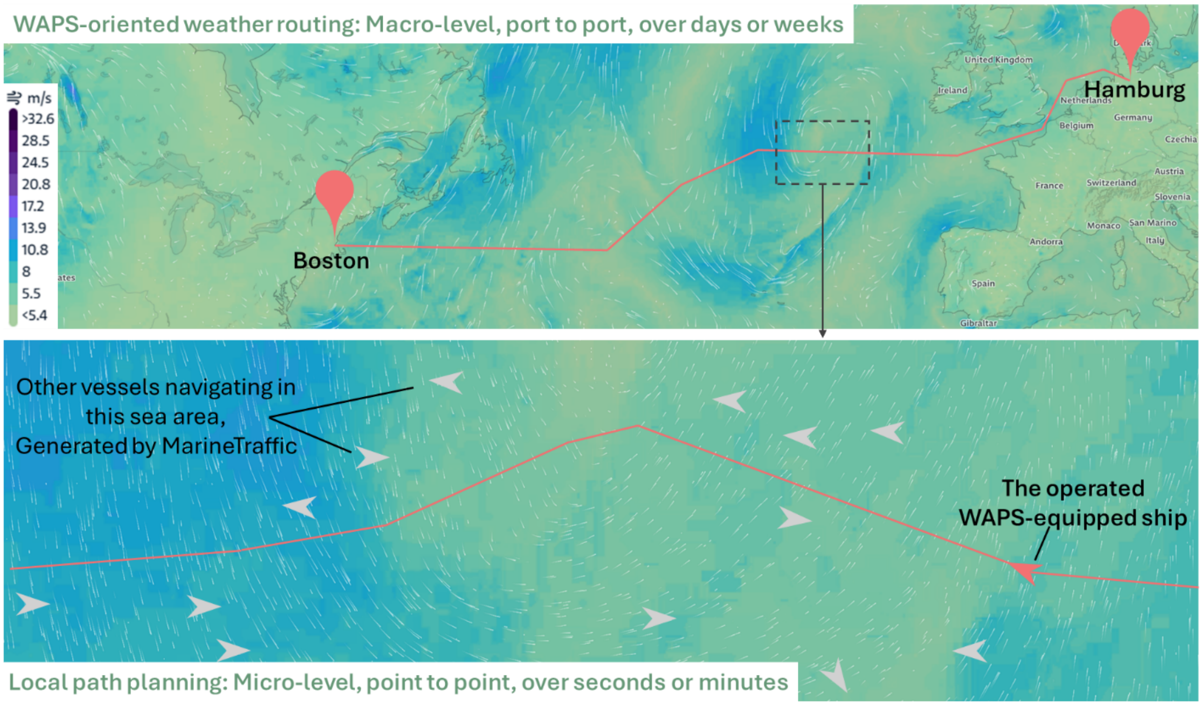

Figure 18 WAPS-oriented weather routing and local path planning for the Hamburg–Boston route.

and emissions while maintaining schedule integrity—based on synoptic-scale meteorological and oceanographic forecasts spanning days or weeks. Ultimately, this methodology optimizes the complex trade-off between maximizing wind-generated thrust and minimizing the hydrodynamic added resistance induced by adverse sea states.

Bentin et al. [159] developed a grid-based A* routing tool calibrated using full-scale measurements from a 17,500 DWT vessel. By coupling wind–wave resistance models with four rotor sails, they demonstrated that WAPS-oriented weather routing outperformed scenarios using either WAPS or weather routing alone. Sun et al. [160] extended the routing framework to three dimensions (longitude, latitude, and speed) and incorporated rotor spin control. Applied to a very large crude carrier (VLCC), the integrated "route–speed–rotor" optimization effectively reduced fuel consumption while maintaining only minor arrival delays.

5.2 Local path planning

Local path planning addresses micro-level, real-time navigation decisions for WAPS-equipped vessels within their immediate operational environment, as shown in Fig. 18. These decisions typically occur within seconds to minutes and ensures operational safety and maximum WAPS functions. Compared with conventional heading control, local path planning must balance additional thrust generated by WAPS against the rudder and heel penalties.

Guzelbulut et al. [161] compared two local guidance strategies under WAPS functions. In a basic heading-keeping mode, the autopilot tracked successive waypoint. Crosswinds cause lateral drift, and reducing waypoint spacing to 100 km decreases detours and yields ~8% fuel savings with WAPSs. In a more advanced course-and-speed mode, the vessel steers toward a virtual leader moving exactly along the planned line, commanding both rudder and engine. The resulting straight track reduces side-slip resistance and travel distance, achieving nearly one-third energy savings under beam winds. In addition, artificial neural networks were explored to enhance the control performance [162]. Liu et al. [163] investigated a segment of the classical route from Malacca to Cape of Good Hope and demonstrated that optimized local path planning reduced fuel consumption by 5.25% even with a 2.3% increase in voyage distance.

Beyond efficiency, local path planning must incorporate obstacle and collision avoidance constraints [164,165]. Coupling real-time WAPS thrust optimization with such safety constraints is therefore a promising research direction.

5.3 Ship motion and maneuverability

WAPSs can influence all six degrees of freedom of a vessel. However, the amplified roll motion caused by aerodynamic heel moments from WAPSs remains a particular concern [68,120,133,134]. The added weight and height of WAPSs increase the vertical center of gravity of vessels, which may reduce stability margins. Dynamic wind loads, including gusts and shifts in direction, introduce irregular accelerations, lateral drift, and yaw; this necessitates rapid responses from the main engine and rudder to maintain course and speed.

WAPSs also impact maneuverability. Drift forces generated by aerodynamic loads can displace the vessel from its intended track even when the bow is aligned with the heading correctly. This demands more frequent and precise rudder adjustments to maintain heading. Turning performance may also be affected [166], with variations in turning circle diameter and initial helm response depending on apparent wind conditions.

Existing studies [132,167] have modeled and predicted ship motion and maneuverability influenced by WAPSs mainly using simplified analytical approaches such as the maneuvering modeling group (MMG) model [168–170], experimentally derived hull hydrodynamics and WAPS aerodynamics, propeller thrust, and Kijima rudder forces [171]. Results show that WAPS-induced side forces primarily affect maneuverability by increasing drift and heel angles, which the rudder can counter without saturation, indicating controllability is maintained. However, more accurate simulations of ship maneuvering with WAPS under real marine wind conditions may yield deeper insights into performance effects and support the development of coordinated control strategies. To accurately capture and utilize these complex real-world environmental factors, advanced sensing technologies are indispensable. For instance, the method pioneered by Shanghai Jiao Tong University establishes a novel paradigm for shipborne wave sensing [172]. It enables, for the first time, non-intrusive real-time wave measurement under coupled sea-state and platform-motion conditions, delivering high-quality real-time wave data and demonstrating significant academic novelty and engineering relevance. Integrating such high-fidelity wave data into motion prediction models will be a critical step forward in evaluating WAPS performance.

5.4 Control of hybrid propulsion systems

As WAPS function only as a supplementary power source and cannot fully replace conventional propulsion systems, coordinated control of hybrid propulsion systems is essential. Such systems integrate main engines with other green alternatives to achieve zero-emission goals [173–178].

However, dynamically managing power distribution across heterogeneous sources remains a major challenge with such systems. Unlike engines or batteries with predictable outputs, wind energy has high variability and increases the complexity of control decisions. The system must continuously determine the amount of propulsion to be provided by engines and the amount of thrust that can be extracted from WAPSs, as well as evaluate the interactions between these sources in real time. Some studies have proposed WAPS–propeller co-control strategies to minimize required propeller thrust and reduce fuel consumption [80,179].

However, maximizing WAPS thrust also considerably increases heel and drift forces (Section 5.3), thereby increasing rudder and thruster demand. This additional control strategy can lead to higher fuel consumption [161,180]. Therefore, more comprehensive propulsion control strategies that balance energy efficiency with stability and maneuverability is required. For example, selecting a slightly lower rotor spin ratio and trimming helm angles can provide an additional 1%–2% fuel savings beyond that achieved using thrust-maximizing strategies alone [161,180].

5.5 Global multiobjective ship–WAPS control

Isolated control strategies for ships equipped with WAPSs are insufficient leverage the decarbonization potential of WAPSs and may introduce safety risks. Therefore, a global multiobjective control framework is required for the successful integration of WAPSs into overall ship operation.

A functional global multiobjective ship–WAPS control framework integrates WAPS-oriented weather routing, local path planning, ship motion and maneuverability, and hybrid propulsion control. Strategic weather routing provides macro-level guidance, which must be executed tactically via micro-level local path planning that accounts for short-term navigation. Both levels must be supported by accurate ship performance models that capture WAPS-induced effects on motion (e.g., dynamic heel moments) and maneuverability (e.g., turning circles). The hybrid propulsion control framework serves as the central coordinator, managing power distribution, WAPS efficiency, and trim optimization based on strategic inputs, real-time data, and performance feedback to satisfy multiple objectives simultaneously.

This tightly coupled and dynamic control task requires advanced decision-support systems, including high-accuracy fuel consumption predictions that account for nonlinear feature interactions, adaptive route-segmentation techniques for practical scenario representation, and multivariable optimization algorithms that can optimize navigation speed, trim, and WAPS control [160,163,181–183]. Moreover, transitioning from a sequential process to a multiobjective parallel process [182], in which routing, propulsion, and WAPS control are reformulated as interacting optimization problems and solved collaboratively, offers a promising pathway toward green shipping.

6 Impact analysis

As a commercial decarbonization technology, WAPSs also entail environmental, economic, social, and political impacts; these aspects are discussed in this section.

6.1 Environmental and economic impacts

The environmental and economic impacts of WAPSs are closely linked because fuel savings directly translate into economic benefits and reductions in GHG emissions. However, comprehensive economic assessment must account for more than fuel savings alone, including costs beyond the operation stage, highlighting the need for comprehensive evaluations such as LCA and LCC methodologies.

6.1.1 LCA and LCC

As shown in Fig. 14, LCA and LCC represent the life cycle environmental and economic impacts of WAPSs, respectively; these assessments are essential for convincing the market, shipowners, and other stakeholders to adopt WAPSs. Prospective assessments require the rapid estimations of WAPS performance, fuel savings, emission reductions, and economic benefits over the system's service lifetime.

An LCA and LCC framework with necessary considerations is shown in Fig. 19. The lifecycles of WAPSs can be divided into three stages: implementation, operation, and decommissioning.

In the implementation stage, WAPS are manufactured and transported to a dry dock for retrofitting onto the vessel. These activities generate additional emissions. From an economic perspective, this stage introduces capital expenditure (CAPEX) that includes retrofitting fees, dry-dock fees, and revenue loss due to refit downtime. Treatment costs for implementation-stage emissions may also apply in some cases. In contrast, government grants or subsidies may partially offset these costs due to the environmental benefits of WAPSs [184,185].

During the operation stage, the primary focus is on evaluating fuel savings over the remaining service life of the vessel. These savings are then used to estimate GHG emission reductions for the LCA framework. Operational expenditure (OPEX) considerations include additional electricity consumption and maintenance costs for WAPS operation. However, reduced engine power leads to lower engine-related OPEX and fuel costs. Potential disadvantages include reduced cargo capacity, which considerably impacts container vessels but has minimal effect on bulk carriers and tankers, due to WAPS occupying deck space (except for kite sails) and longer voyage durations caused by optimized routing or

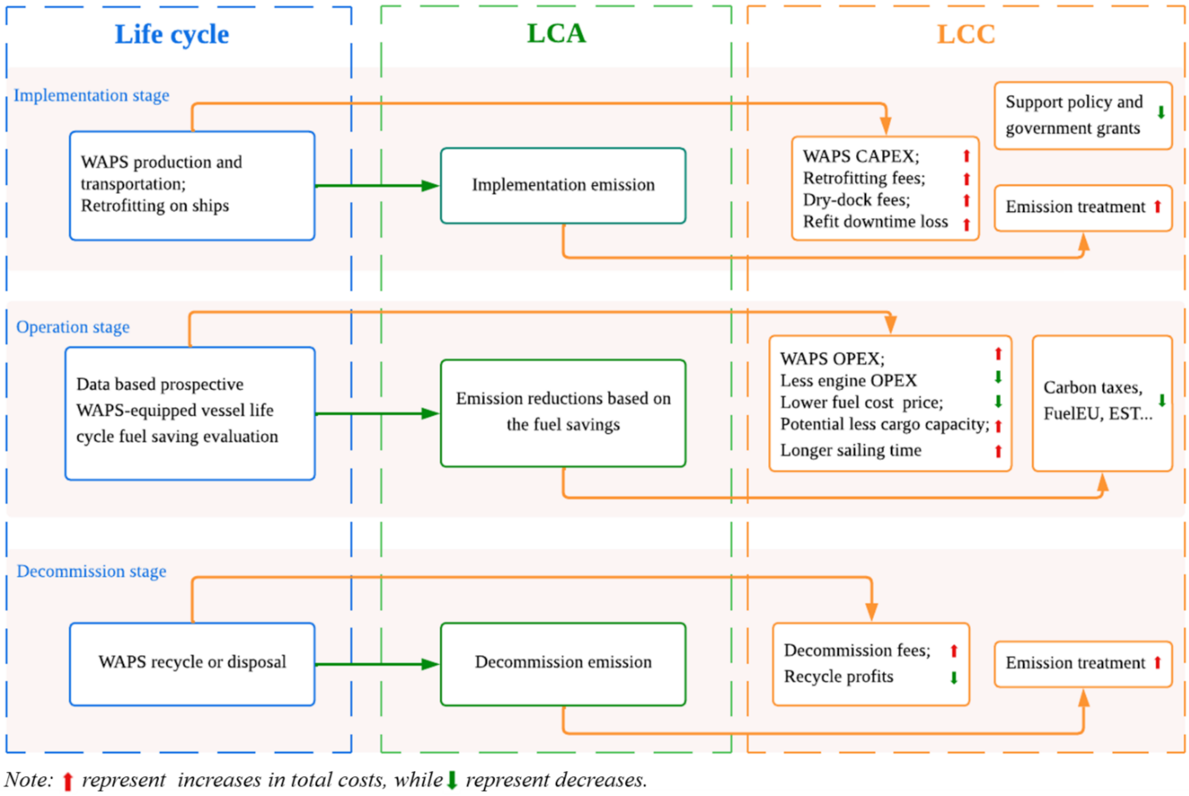

Figure 19 WAPS LCA and LCC framework.

reduced speed, which may result in profit loss. In contrast, reduced emissions reduce carbon-related costs such as those imposed by FuelEU and EU ETS.

At the end of their lifecycle, WAPSs are decommissioned, ideally at the same time as the host vessel for optimal reliability and profits. This stage generates decommissioning-related emissions and disposal costs. If the system or components can be recycled, some investment can be recovered via salvage value.

6.1.2 Existing evaluation frameworks

Within the LCA and LCC processes for WAPSs, the most challenging task is to accurately and rapidly estimate the fuel savings during preliminary design based on limited input data and existing empirical knowledge [186,187]. Despite these constraints, several studies have proposed rapid evaluation frameworks (Table 6). These frameworks are based on existing WAPS performance databases, marine wind datasets, and simplified methodologies for detecting ship motion and fuel consumption. These frameworks usually consider a single route or the lifetime navigation, with a focus on evaluating the environmental impacts of WAPSs during the operational stage.

These studies primarily focused on the operation stage and estimated fuel savings and GHG reductions via the simplified modeling of ship–WAPS interactions. Thus, they addressed only a part of the full LCA and LCC framework. Among these approaches, the in-house code ShipCLEAN [122,177,178,196–200] stands out as a representative sample. Leveraging CFD and experimental databases, its WAPS module predicts aerodynamic performance. When integrated with the ship static and engine module and economic evaluation module, ShipCLEAN enables assessing fuel savings and overall profitability associated with WAPS implemenation.

Another remarkable tool is the Flettner Rotor Savings Estimator (Fig. 20), which was specifically designed by LR to estimate propulsion fuel savings and emission reductions for rotor sail installations. This estimator accounts for variables such as ship type, size, velocity, and loading; rotor configuration and layout; and navigation route and season, offering a practical reference for preliminary design. Norsepower also developed a similar tool known as Simplified Performance Simulator.

6.1.3 Industrial measurements of fuel savings

Accurately measuring the fuel savings achieved by WAPS is challenging but highly valuable, as such measurements provide the foundation for developing and validating LCA and LCC frameworks and related estimations. With the rapid growth of the WAPS market and increasing demonstration applications, industry stakeholders have been reporting actual fuel savings measured from long-term practical navigation, as summarized in Table 7.

An analysis of these measurements across varying WAPS configurations and navigational conditions revealed that the actual fuel savings were typically below 10%, considerably lower than the idealized 20% savings often claimed via numerical studies and scaled tests. The discrepancy is primarily due to the complexity of real marine environments and operational uncertainties during WAPS usage. This highlights the importance of performance simulations under realistic conditions and the need to develop a multiobjective ship–WAPS control system, as discussed in Section 4.3.3 and Section 5.5, respectively. To further bridge this gap, standardized validation protocols and digital twin technologies can be developed. These advancements will enable dynamic comparison between onboard sensor data and theoretical or empirical models, ensuring that projected efficiency gains are reliably translated into operational reality.

Table 6 Summary of existing studies on the environmental and economic impact assessment of WAPSs

Ref.	WAPS type	Ship information	Core tool & method	Key input data	Economic factors	Key output data
Talluri et al. 2018 [188]	Rotor sails × 3	RoRo	TERA framework; in-house TURBOMATCH code	Holtrop calm water and wave resistance; rotor sails thrust from [83]; engine SFOC; and COGOW wind database	Fuel price; CAPEX & OPEX; carbon taxes; actualized cost	Fuel savings; GHG reduction; payback years
Zhang et al. 2021 [185]	Rotor sails × 2; Kite sail	Bulker (Lpp 194.5 m)	TERA framework	Engine SFOC; UKHO wind database; rotor sails thrust from Norsepower; and kite sails thrust from Skysail	Fuel price; ship OPEX; WAPS CAPEX & OPEX	Fuel savings; payback years
Lindstad et al. 2022 [189]	Rotor sails × 4	Bulker (LOA 200 m, B 32.3 m)	TCE cost model; power balance model; and NAPA hull variants tool	Weibull wind database; Holtrop calm water and STA wave resistance; rotor sails thrust from [122]; and engine SFOC	Annualized CAPEX & OPEX; fuel price; carbon taxes	Fuel savings; GHG reduction; annual costs
Angelini et al. 2023 [190]	Rotor sails × 2	RoRo (Lpp 135 m, B 22.5 m, D 7 m)	Matlab; Maritime DelftShip; Dijkstra's algorithm; and 6-DOF resistance and maneuvering model	NOAA wind database; ship hydrostatics; rotor sails thrust from wind tunnel; and engine propulsion	Rotor CAPEX & OPEX; dry-dock fee; refit downtime; fuel price; carbon taxes; engine CAPEX	Fuel savings; GHG reduction; rotor-engine power split; payback years
Ghorbani et al. 2023 [191]	BLC sails × 2	Container ship (LOA 118.19 m, B 13.35 m, D 3–6.2 m)	Python; Dynamic 4-DOF solver with heading controller; and PPP polar analysis	CDS ERA5 wind and wave database; ship hydrostatics and resistance; BLC sails thrust from technology provider; logged propeller pitch/RPM; engine SFOC; and sensor logs (power, fuel, and GPS)	N/A	Route SOG; engine brake power; fuel savings; GHG reduction; equivalent WAPS power
Alkhaledi et al. 2023 [175]	Rotor sails × 6	LH2 tanker (LOA 370 m, B 75 m, D 35 m)	In-house TURBOMATCH code and Poseidon voyage simulator; TERA framework	COGOW wind database; Holtrop calm water and wave and wind resistance; rotor sails thrust from [122]; and operating time and season sea states	Combination with LH2 fuel	Fuel savings; GHG reduction; overall thermal efficiency
Ma et al. 2023 [192]	Wing sails × 4	VLCC tanker (LOA 332.95 m, B 60 m, D 30 m)	MMG-based 3-DOF ship model; rudder balance; and power balance model	Wing sails thrust from wind tunnel; CDS ERA5 wind database; route; and engine power curve	N/A	Wing sail power production; fuel savings
Reche Vilanova et al. 2024 [193]	Digital WAPS (Directly give thrust)	Bulker (LOA 292 m, B 45 m, D 16.5 m)	Power balance model	Ship hydrostatics; engine SFOC; and propeller control strategy	Fuel price; carbon taxes; CAPEX & OPEX	Fuel savings; payback year; NPV
Saettone et al. 2025 [51]	BLC sails × 4	Chemical tanker (LOA 183.07 m, B 32.2 m)	3-DOF static solver; power balance model; panel method; and CII calculator	BLC thrust from bound4blue; AIS/GPS track; Copernicus wind database; and engine SFOC	N/A	GHG reduction; CII
Čalić et al. 2024 [194]	Wing sails × 3	Container ship (LOA 363 m, B 45.6 m)	Python and power balance model	Engine SFOC; Copernicus Marine Services wind database; and propeller propulsion	N/A	Fuel savings
Guzelbulut et al. 2024 [195]	Rotor sails and Wing sails × 10	KVLCC2 tanker (Lpp 320 m, B 58 m, D 20.8 m)	Matlab; MMG-based 3-DOF ship model; rudder and propeller controllers	Ship hydrodynamics; wind and Beaufort-scaled wave database; NACA0015 wing sail thrust; and rotor sails thrust from [122]	N/A	Fuel savings
ShipCLEAN 2019–2025 [122,177,178, 196–200]	Rotor sails and Wing sails; Multiple units	MR tanker; container ship; ferry; RoRo	In-house code ShipCLEAN (Matlab); Dynamic 4-DOF solver	Ship hydrostatics and resistance; engine and propeller propulsion; WAPS thrust from CFD and experiments; engine SFOC; wind, wave, and current database; and route	WAPS CAPEX & OPEX; Psaraftis cost-income model [201]; fuel price; Norsepower cost database	Fuel savings; GHG reduction; involuntary speed loss; payback years
Ammar et al. 2025 [174]	Rotor sails × 6	LNG carrier (LOA 280.96 m, B 44.04 m, D 12.52 m)	Power balance model and IMO EEXI & CII calculators	Meteoblue weather statistics; rotor sails thrust from Norsepower; and engine SFOC	Annual CAPEX & OPEX; fuel price; carbon taxes; combination with natural gas	Fuel savings; GHG reduction; EEXI & CII; LCOE

Note: B, breadth on water line; CDS, Copernicus Climate Data Store; COGOW, Climatology of Global Ocean Winds; D, ship's mean draft; DOF, degree-of-freedom; LCOE, levelized cost of electricity; Lpp, ship design length between perpendiculars; LOA, ship's length overall; NOAA, The US National Oceanic and Atmospheric Administration; NPV, net present value; PPP, performance prediction plot; SFOC, specific fuel oil consumption of the engine; SOG, speed over ground; TCE, daily time charter equivalent cost; TREA, techno-economic environmental risk analysis.

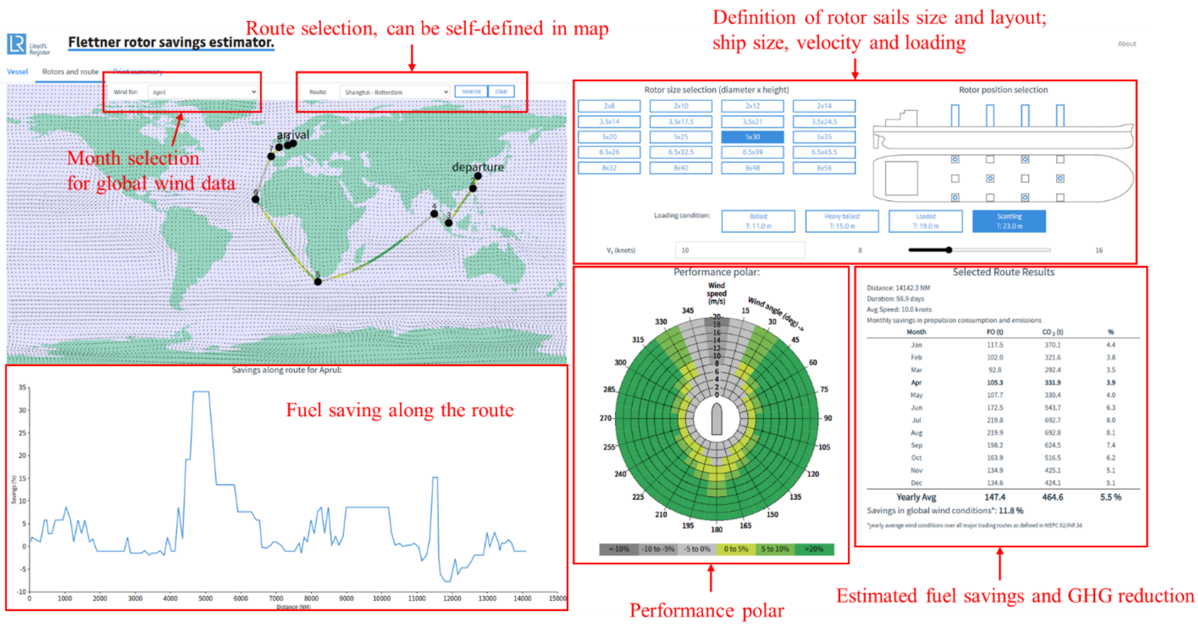

Figure 20 User Interface of LR rotor savings estimator. Produced using the Energy Technologies Institute's Flettner Rotor System Tool developed by Lloyd's Register, sub-licensed to this work by Lloyd.

Table 7 Fuel savings from practical navigation of vehicles equipped with WAPS

Ship	WAPS	Main navigation route or region	Fuel savings
E-ship 1 [202]	Rotor sails × 4	North and Baltic Sea, North and South Atlantic Ocean and the Mediterranean Sea	15%
M/V Estraden [39,203]	Rotor sails × 2	Teesport in the UK and Zeebrugge in Belgium	6.1%
M/V Copenhagen; M/V Berlin [204]	Rotor sails × 1	Rostock in Germany to Gedser in Denmark	4%
M/S Viking Grace [39]	Rotor sails × 1	Baltic sea	231–315 t annually
Maersk Pelican [205]	Rotor sails × 2	Europe, Middle East, Asia and Australia	8.2%
M/V Annika Braren [206]	Rotor sails × 1	North sea	2%–4.5%
M/V Afros [39]	Rotor sails × 4	Nantong in China to Vancouver in Canada	12.5%
M/T Sea Zhoushan [39]	Rotor sails × 5	Pacific Ocean, China to Brazil	8%
M/V Pyxis Ocean [207]	Wing sails × 2	Indian Ocean, Pacific Ocean, North and South Atlantic	14%
M/V Berge Olympus [208]	Wing sails × 4	Pacific Ocean, China to Brazil	Average 6 t per day
M/V Frisian Sea [209]	BLC sails × 2	North and Baltic Sea, North Atlantic Ocean	2.0%–3.3%
Ville de Bordeaux [210]	BLC sails × 3	North Atlantic Ocean, Europe to the US	568 t annually
MS Onego Deusto [211]	Kite sails × 1	Germany to Venezuela	15%–20%

6.2 Social and political impacts

As an emerging renewable decarbonization technology, WAPSs inevitably carry social and political implications and are subject to scrutiny from both the public and governments. Effective engagement with these stakeholders can accelerate the adoption and acceptance of WAPSs; failure to do so may place the technology in a development dilemma [212].

6.2.1 Social acceptance

The social acceptance of WAPSs depends on three main factors: (1) public perception of energy sources, (2) potential impacts on health, and (3) positive contributions to society and the economy.

First, WAPSs benefit from favorable public perception toward the adoption of wind energy. Unlike other alternative renewable energy sources such as hydrogen [213,214], nuclear [215,216], or certain fuel cells [217], which often face skepticism or safety concerns, wind energy is widely accepted and recognized as clean and mature [218,219]. This perception is reflected in the global deployment of wind turbines and sustained public support [124,220,221].

Second, WAPSs offer environmental advantages for marine ecosystems by producing fewer emissions and underwater noise and posing less risk to marine life compared with conventional propulsion systems [222,223]. For onboard crew, potential aerodynamic noise by WAPSs may require further investigation to ensure occupational safety. WAPSs also contribute to improved regional air quality along shipping lanes, contributing to public health improvements in coastal and port areas [224,225].

Third, social welfare and employment impacts considerably influence public acceptance of WAPSs. As a retrofittable and newbuild-compatible technology, WAPSs stimulate demand for specialized talents in this field and create jobs. Considering the cyclical nature of the shipbuilding industry [226], which experiences significant fluctuations in employment and investment, the integration of WAPSs can provide new vitality and long-term growth.

6.2.2 Supportive policy

As an environmentally policy-driven technology with potential economic benefits, the adoption of WAPSs ultimately depends on shipowners' investment decisions. If the LCC evaluation fails to demonstrate economic viability from the owner's perspective, WAPS deployment will encounter significant barriers.

In this context, financial support policies play a critical role. By directly offsetting retrofit costs and shortening payback periods, such measures can improve the market viability of WAPSs [184,185]. Examples include incentivizing shipowners via tax breaks, subsidies, and low-interest loans; increasing carbon taxes while offering financial returns or credits for low-emission WAPS-equipped ships; and establishing long-term policy frameworks with clear targets and timetables for WAPS adoption to provide investment certainty.

To maximize the effectiveness of supportive financial policies, limited funds should not be distributed uniformly across all eligible vessels. Instead, support can be strategically directed toward ships that occupy central positions within the industry's social network and exert strong peer influence [184,227,228]. In addition, for unprofitable but essential routes—such as domestic shipping in Fiji—WAPSs present a viable solution to reduce financial burdens and maintain service continuity [229].

6.2.3 Uncertainties due to geopolitical situations

Geopolitical conflicts, such as the Red Sea turmoil and Middle East tensions [230–232], has exposed the shipping industry to heightened risks, including volatile oil prices and costly rerouting. In this context, WAPSs can enhance operational resilience, moving beyond environmental benefits.

By harnessing wind energy, WAPSs reduce dependence on fossil fuels, hedges against oil price volatility, and generates direct cost savings during oil price spikes. When vessels are required to take longer detours around chokepoints such as the Suez Canal, WAPSs combined with advanced weather routing can help ships optimize wind resource utilization. This can mitigate additional fuel consumption and costs of longer voyages as well as enhance energy security by diversifying power sources. Ultimately, WAPSs fortify the shipping industry against uncertain geopolitical conditions and ensure greater stability.

7 Future outlook

The WAPS market has experienced accelerated growth along with increased acceptance among society and shipowners. Despite recent developments, several challenges remain such as inadequate propulsion efficiency, uncertain operational safety, insufficient economic assessments, and lack of standards and policy frameworks. To foster a more reliable and scalable market, nine specific research topics are proposed below that can guide future studies.

1. Design and aerodynamic optimization of high-lift and kite concepts

Among all WAPSs, rotor and wing sails are approaching their practical upper limits due to geometric dimension limits. In contrast, BLC and kite sails present considerable untapped potential. In principle, BLC sails can achieve higher aerodynamic coefficients via improved BLC, whereas kite sails can enhance performance by increasing the effective kite area at high altitudes; both these improvements can be achieved without introducing significant additional disturbances to the ship. For BLC sails, future research should focus on optimizing the energy balance between the internal suction power consumption and aerodynamic lift gain. For kite sails, the primary challenge lies in the automation of launch and recovery cycles under adverse weather conditions. Research into dynamic flight trajectory optimization must be conducted to maximize crosswind power generation.

2. Holistic layout optimization of WAPS arrays

As ships deploy multiple WAPS units to maximize power, aerodynamic interaction effects (e.g., wake shading) become critical. Current layouts are typically arranged in regular configurations and operated without dedicated compromise strategies. However, several studies have shown that the overall system performance can be improved by adopting special heuristic layouts. Future studies should employ multiobjective optimization algorithms to determine layouts that minimize aerodynamic interference while satisfying strict constraints related to vessel stability, visibility, and deck operations.

3. Design standardization

Although several standards and guidelines have been published by various classification societies, many of their provisions are general. Much of the content refers to general shipbuilding requirements without specifically addressing the unique characteristics and operational needs of WAPSs. Therefore, detailed standards must be developed for WAPSs to facilitate their large-scale adoption.

4. Integrated ship–WAPS control systems

At present, WAPSs only serve as a supplementary energy source and must be integrated with conventional diesel engines or other renewable alternative fuels. Treating WAPSs as isolated subsystems limits their effectiveness. Instead, the industry should transition toward a global multiobjective parallel ship–WAPS control system. This transition requires replacing reactive control strategies with predictive control that integrates real-time weather routing, engine load management, and WAPS settings. The goal is to optimize the total ship emission index (EEXI/CII) rather than just the thrust of the sails.

5. WAPS structural safety and health monitoring

WAPS are tall, slender structures exposed to substantial wind and fatigue loads, and kite sails face tether failure risks. Concurrently, without structural health monitoring during operation, onboard crew cannot make informed decisions. Future research should integrate Internet of Things (IoT)-based sensors (strain gauges and accelerometers) to build structural digital twins. Such systems will enable predictive maintenance and the early detection of tether degradation (in kites) or bearing fatigue (in rotors) before catastrophic failure occurs.

6. Maneuverability and collision avoidance

WAPS integration considerably impacts ship maneuverability, including course-keeping and turning ability; additionally, component failures may pose secondary issues. Research is needed to quantify these impacts under IMO maneuverability standards. Furthermore, collision avoidance algorithms must be updated and integrated with global control to account for maneuvering constraints and blind spots introduced by large sail arrays, thereby ensuring navigational safety while capturing efficiency gains.

7. Data-driven performance evaluation

A significant discrepancy exists between numerical or scaled experimental predictions and sea-trial results. Simplified WAPS simulations often neglect real-world factors such as complex marine environments and ship–WAPS coupling, leading to overestimated performance. To address this discrepancy, high-fidelity models must be developed and open-source databases of full-scale operational data must be systematically built. Research should also focus on developing data-driven models that can correct low-fidelity fast simulations, thereby reducing investment uncertainty for shipowners.

8. Comprehensive lifecycle impact assessment

Beyond fuel savings, current environmental and economic assessments often overlook the full life cycle of WAPSs. Comprehensive LCA and LCC analyses must be conducted to quantify total carbon footprint and economic performance, particularly payback periods, by considering pricing sensitivity (e.g., EU ETS prices); this will enable transparent and credible analysis of the said factors.

9. Policy intervention

Stronger policy interventions are essential to accelerate WAPS deployment. Policy-related research should move beyond general advocacy, and quantitative studies must be conducted to determine the tipping points of carbon pricing that make specific WAPS technologies viable for different ship segments. Financial incentives can also reduce investment risks, whereas targeted policy support, particularly the promotion of successful demonstration projects, can provide credible reference cases for broader industry adoption of WAPSs.

8 Conclusion

This comprehensive techno-economic review of WAPS presents a class of key technologies for promoting green shipping. The key research questions outlined in the introduction have been addressed via in-depth analysis. The main conclusions are summarized below:

1) WAPSs can be broadly categorized into rotor sails, BLC sails, wing sails, and kite sails based on their aerodynamic characteristics. Rotor sails rely on the Magnus effect, BLC sails apply active BLC technology, wing sails primarily exploit their section shapes and AOA, and kite sails maximize lift via active dynamic crosswind trajectories that increase the relative velocity between the wind and kite.

2) Among the four WAPS types, wing sails have garnered the greatest academic interest, whereas rotor sails and BLC sails currently show stronger market interest. Kite sails remain at a relatively low TRL of 3–7, requiring further development before large-scale application. In terms of ultimate propulsion efficiency, BLC and kite sails are expected to demonstrate higher aerodynamic performance.

3) The design of WAPSs inherently involves trade-offs among safety, propulsion efficiency, and cost. The complete design process is divided into four stages, namely design inputs, preliminary design, detailed design, and finalization, and critical considerations are addressed at each stage.

4) The integration of WAPSs into ships has introduced new operational challenges such as the need for improvements in weather routing and local path planning, considerations of ship motion and maneuverability, and the potential development of a global multiobjective ship–WAPS control system. Such a system is expected to achieve the dual objectives of ensuring operational safety while maximizing propulsion efficiency.

5) WAPS will generate economic and environmental benefits, primarily via fuel savings and reduction in GHG emissions. Existing assessment studies have been reviewed, and their limitations are identified. To further stimulate WAPS adoption, comprehensive LCA and LCC assessment frameworks are proposed and relevant tools are compiled to support future research. In addition, the social and political impacts of WAPSs are analyzed, which are expected to provide additional incentives for their market uptake.

Acknowledgements

None.

Author contribution statement

Wenzhe Zhang: Writing – original draft & review & editing, Conceptualization, Data curation, Formal analysis, Methodology, Visualization; **Zhiyu Jiang:** Writing – review & editing, Formal analysis; **Javier Calderon-Sanchez:** Writing – review & editing, Funding acquisition; **Lisa Martínez:** Writing – review; **Simone Saettone:** Writing – review; **H. Bill Galdós-Lindao:** Writing – review; **Jordi Mas-Soler:** Writing – review.

Data availability

Data will be provided upon request.

Declaration of competing interest

All the contributing authors report no conflicts of interest in this work.

Funding

This research has been funded by the Ministry of Science, Innovation and Universities (MCIU) of Spain under the project FOWTDAMP2 (Grant No. PID2021-123437OB-C21), and project RENEWFLOAT (Grant No. PID2024-161775OB-C21).

Use of AI statement

None.

References

[1] Wang, F., Harindintwali, J. D., Yuan, Z. Z., Wang, M., Wang, F. M., Li, S., Yin, Z. G., Huang, L., Fu, Y. H., Li, L., et al. (2021). Technologies and perspectives for achieving carbon neutrality. *Innovation* 2, 100180.

[2] Wei, M. Y., Chen, K. Y., Kang, J. N., Chen, W. M., Wang, X. Y., Zhang, X. Y. (2022). Policy and management of carbon peaking and carbon neutrality: a literature review. *Engineering* 14, 52–63.

[3] Faber, J., Hanayama, S., Pereda, P., Comer, B., Hauerhof, E., Loeff, W. S. van der, Smith, T., Zhang, Y., Kosaka, H., Adachi, M., et al. (2021). Fourth Greenhouse Gas Study 2020. London, UK: International Maritime Organization.

[4] International Maritime Organization (2023). 2023 IMO strategy on reduction of GHG emissions from ships. Report, IMO.

[5] Christodoulou, A., Cullinane, K. (2022). Potential alternative fuel

pathways for compliance with the 'FuelEU Maritime Initiative'. *Transp. Res. Part D: Transp. Environ.* 112, 103492.
[6] Kondratenko, A. A., Zhang, M. Y., Tavakoli, S., Altarriba, E., Hirdaris, S. (2025). Existing technologies and scientific advancements to decarbonize shipping by retrofitting. *Renew. Sustain. Energy Rev.* 212, 115430.
[7] Tadros, M., Ventura, M., Guedes Soares, C. (2023). Review of the decision support methods used in optimizing ship hulls towards improving energy efficiency. *J. Mar. Sci. Eng.* 11, 835.
[8] Lindstad, E., Bø, T. I. (2018). Potential power setups, fuels and hull designs capable of satisfying future EEDI requirements. *Transp. Res. Part D: Transp. Environ.* 63, 276–290.
[9] Davidson, I., Scianni, C., Hewitt, C., Everett, R., Holm, E., Tamburri, M., Ruiz, G. (2016). Mini-review: assessing the drivers of ship biofouling management–aligning industry and biosecurity goals. *Biofouling* 32, 411–428.
[10] Valchev, I., Coraddu, A., Kalikatzarakis, M., Geertsma, R., Oneto, L. (2022). Numerical methods for monitoring and evaluating the biofouling state and effects on vessels' hull and propeller performance: a review. *Ocean Eng.* 251, 110883.
[11] Zhen, L., Hu, Z., Yan, R., Zhuge, D., Wang, S. A. (2020). Route and speed optimization for liner ships under emission control policies. *Transp. Res. Part C: Emerg. Technol.* 110, 330–345.
[12] Jimenez, V. J., Kim, H., Munim, Z. H. (2022). A review of ship energy efficiency research and directions towards emission reduction in the maritime industry. *J. Cleaner Prod.* 366, 132888.
[13] Han, Y. Y., Ma, W. H., Ma, D. F. (2023). Green maritime: an improved quantum genetic algorithm-based ship speed optimization method considering various emission reduction regulations and strategies. *J. Cleaner Prod.* 385, 135814.
[14] Yu, H. C., Fang, Z. X., Fu, X. J., Liu, J. X., Chen, J. H. (2021). Literature review on emission control-based ship voyage optimization. *Transp. Res. Part D: Transp. Environ.* 93, 102768.
[15] Hoang, A. T., Foley, A. M., Nižetić, S., Huang, Z. H., Ong, H. C., Ölçer, A. I., Pham, V. V., Nguyen, X. P. (2022). Energy-related approach for reduction of CO_2 emissions: a critical strategy on the port-to-ship pathway. *J. Cleaner Prod.* 355, 131772.
[16] Zhao, J. X., Wei, Q. F., Wang, S. S., Ren, X. L. (2021). Progress of ship exhaust gas control technology. *Sci. Total Environ.* 799, 149437.
[17] Hua, W. S., Sha, Y. S., Zhang, X. L., Cao, H. F. (2023). Research progress of carbon capture and storage (CCS) technology based on the shipping industry. *Ocean Eng.* 281, 114929.
[18] Pancione, E., Erto, A., Di Natale, F., Lancia, A., Balsamo, M. (2024). A comprehensive review of post-combustion CO_2 capture technologies for applications in the maritime sector: a focus on adsorbent materials. *J. CO_2 Util.* 89, 102955.
[19] Lion, S., Vlaskos, I., Taccani, R. (2020). A review of emissions reduction technologies for low and medium speed marine Diesel engines and their potential for waste heat recovery. *Energy Convers. Manage.* 207, 112553.
[20] Zhu, S. P., Zhang, K., Deng, K. Y. (2020). A review of waste heat recovery from the marine engine with highly efficient bottoming power cycles. *Renew. Sustain. Energy Rev.* 120, 109611.
[21] Singh, D. V., Pedersen, E. (2016). A review of waste heat recovery technologies for maritime applications. *Energy Convers. Manage.* 111, 315–328.
[22] Hansen, J. F., Wendt, F. (2015). History and state of the art in commercial electric ship propulsion, integrated power systems, and future trends. *Proc. IEEE* 103, 2229–2242.
[23] Li, R., Li, H., Huang, W. T., Tao, H. Q., Xu, W. W., Tai, N. L., Li, C. B. (2025). Accelerating green shipping with spatially optimized offshore charging stations. *Nat. Energy* 10, 243–254.
[24] Guo, S. Q., Wang, Y. B., Dai, L., Hu, H. (2023). All-electric ship operations and management: overview and future research directions. *Etransportation* 17, 100251.
[25] Nivolianiti, E., Karnavas, Y. L., Charpentier, J. F. (2024). Energy management of shipboard microgrids integrating energy storage systems: a review. *Renew. Sustain. Energy Rev.* 189, 114012.
[26] Geertsma, R. D., Negenborn, R. R., Visser, K., Hopman, J. J. (2017). Design and control of hybrid power and propulsion systems for smart ships: a review of developments. *Appl. Energy* 194, 30–54.
[27] Wu, N. Y., Zhang, F., Zhang, F. Z., Jiang, C. X., Lin, J., Xie, S., Jing, R., Zhao, Y. R. (2024). An integrated multi-objective optimization, evaluation, and decision-making method for ship energy system. *Appl. Energy* 373, 123917.
[28] Pan, P. C., Sun, Y. W., Yuan, C. Q., Yan, X. P., Tang, X. J. (2021). Research progress on ship power systems integrated with new energy sources: a review. *Renew. Sustain. Energy Rev.* 144, 111048.
[29] Deniz, C., Zincir, B. (2016). Environmental and Economical assessment of alternative marine fuels. *J. Cleaner Prod.* 113, 438–449.
[30] Atilhan, S., Park, S., El-Halwagi, M. M., Atilhan, M., Moore, M., Nielsen, R. B. (2021). Green hydrogen as an alternative fuel for the shipping industry. *Curr. Opin. Chem. Eng.* 31, 100668.
[31] Van Biert, L., Godjevac, M., Visser, K., Aravind, P. V. (2016). A review of fuel cell systems for maritime applications. *J. Power Sources* 327, 345–364.
[32] Chou, T., Kosmas, V., Acciaro, M., Renken, K. (2021). A comeback of wind power in shipping: an economic and operational review on the wind-assisted ship propulsion technology. *Sustainability* 13, 1880.
[33] Mahmoudi, M., Saboohi, Y., Köhler, J. (2024). Facilitating the transition to sustainable propulsion in the shipping industry: an agent-based modelling analysis of retrofitting. *Environ. Innovation Soc. Transitions* 51, 100838.
[34] McGrail, S. (2001). Boats of the World: From the Stone Age to Medieval Times. Oxford: Oxford University Press.
[35] Kelly, M., Gráda, C. Ó. (2019). Speed under sail during the early industrial revolution (c. 1750-1830). *Econ. Hist. Rev.* 72, 459–480.
[36] Griffiths, D. (1993). Triple expansion and the first shipping revolution. In The Advent of Steam: The Merchant Steamship before 1900. Gardiner, R., Greenhill, B., Eds. London: Conway Maritime Press Ltd., p 106–126.
[37] Graham, G. S. (1956). The ascendancy of the sailing ship 1850-85. *Econ. Hist. Rev.* 9, 74–88.
[38] Talluri, L., Nalianda, D. K., Kyprianidis, K. G., Nikolaidis, T., Pilidis, P. (2016). Techno economic and environmental assessment of wind assisted marine propulsion systems. *Ocean Eng.* 121, 301–311.
[39] Laursen, R., Patel, H., Sofiadi, D., Zhu, R., Nelissen, D., Van Seters, E., Pang, D. (2023). Potential of wind-assisted propulsion for shipping. Report, European Maritime Safety Agency.
[40] Patel, C. S. (2024). Energy efficiency retrofit report 2024: applying wind-assisted propulsion to ships. Report, Lloyd's Register.
[41] Hasso, H., Uwe, H., Johanna, T., Kjersti, A., Ola, G. S., Øyvind, E. (2025). Wind-assisted propulsion systems (WAPS)-how WAPS can help to comply with GHG regulations. Report, DNV.
[42] ABS (2025). Wind propulsion technologies. Report, ABS.
[43] Cherubini, A., Papini, A., Vertechy, R., Fontana, M. (2015). Airborne wind energy systems: a review of the technologies. *Renew. Sustain. Energy Rev.* 51, 1461–1476.
[44] Kolodziejski, M., Sosnowski, M. (2025). Review of wind-assisted propulsion systems in maritime transport. *Energies* 18, 897.
[45] Wang, K., Li, Z. W., Liu, X., Hu, Z. Q., Huang, L. Z., Song, Q. S., Liang, H. Z., Jiang, X. L. (2025). Wind-assisted propulsion system for shipping decarbonization: technologies, applications and challenges. *Energy* 336, 138420.
[46] Feng, L. X., Sun, Y. W., Tang, X. J., Yuan, C. Q., Yin, H. B., Luo, W. J. (2026). Review on the development and challenges of clean energy sources for ships. *Renew. Sustain. Energy Rev.* 225, 116181.
[47] Clayton, B. R. (1985). BWEA initiative on wind assisted ship

propulsion (WASP). *J. Wind Eng. Ind. Aerodyn.* 19, 251–276.
[48] Seifert, J. (2012). A review of the Magnus effect in aeronautics. *Prog. Aerosp. Sci.* 55, 17–45.
[49] Magnus, G. (1852). Ueber die Abweichung der Geschosse nebst einem Anhange: Ueber eine auffallende Erscheinung bei rotirenden Körpern: Gelesen in der Akad. *d. Wiss. am 7 Aug. 1851 u. 17 Jun.* 1852, Dümmler.
[50] bound4blue (2024). Aerodynamic optimization of the eSAIL®: advancing wind-assisted propulsion. https://bound4blue.com/aerodynamic-optimization-of-the-esail/ (accessed 14 July 2025).
[51] Saettone, S., Vilanova Vidal, E., Batalha Guerra, N., Zamora, J. (2025). eSAILs®: Using wind to improve real vessel CII and environmental performance. Report, Bound4Blue.
[52] Bordogna, G., Muggiasca, S., Giappino, S., Belloli, M., Keuning, J. A., Huijsmans, R. H. M., van't Veer, A. P. (2018). Wind-tunnel experiments on a large-scale Flettner rotor. In *Proceedings of the XV Conference of the Italian Association for Wind Engineering*. Cham, Germany, p 110–123.
[53] Hopes, W. C. P., Pearson, D. R., Buckingham, J. E. (2021). A CFD study on wind assisted propulsion technology for commercial shipping. In *Proceedings of the RINA Wind Propulsion Conference*. London, UK, p 1–8.
[54] Low, H. T., Luo, S. C., Winoto, S. H. (1991). Flow past a wind-assisted ship propulsion device. *Ocean Eng.* 18, 555–565.
[55] Hcini, C., Abidi, E., Kamoun, B., Afungchui, D. (2016). Numerical prediction for the aerodynamic performance of Turbosail type wind turbine using a vortex model. *Energy* 109, 287–293.
[56] Cairns, J., Vezza, M., Green, R., MacVicar, D. (2021). Numerical optimisation of a ship wind-assisted propulsion system using blowing and suction over a range of wind conditions. *Ocean Eng.* 240, 109903.
[57] Li, Z. Y., Tang, J. (2024). Circulation-controlled wind-assisted ship propulsion: Technical innovations for future shipping industry decarbonization. *Energy Convers. Manage.* 319, 118976.
[58] NASA (2024). NACA airfoils. https://www.nasa.gov/image-article/naca-airfoils/. (accessed 4 June 2025).
[59] Guzelbulut, C., Badalotti, T., Suzuki, K. (2024). Optimization techniques for the design of crescent-shaped hard sails for wind-assisted ship propulsion. *Ocean Eng.* 312, 119142.
[60] Zhang, R., Huang, L. Z., Peng, G. S., Ma, R. Q., Wang, K., Tian, F., Song, Q. S. (2023). A novel method of desynchronized operation of sails for ship wind-assisted propulsion system. *Ocean Eng.* 288, 115964.
[61] Zeng, Q. S., Zhang, X. Y., Cai, W., Zhou, Y. (2023). Wake distortion analysis of a dynarig and its application in a sail array design. *Ocean Eng.* 278, 114341.
[62] Yasuda, A., Taniguchi, T., Katayama, T. (2024). Numerical investigation of aerodynamic interactions between rigid sails attached to ship. *J. Mar. Sci. Eng.* 12, 1425.
[63] Zhu, H., Yao, H. D., Thies, F., Ringsberg, J. W., Ramne, B. (2023). Propulsive performance of a rigid wingsail with crescent-shaped profiles. *Ocean Eng.* 285, 115349.
[64] Zhu, H., Chernoray, V. G., Ringsberg, J. W., Yao, H. D., Ramne, B. (2024). Fluid-structure interaction analysis of crescent-shaped wingsails. In *Proceedings of the 43rd International Conference on Ocean, Offshore and Arctic Engineering*. Singapore, Singapore.
[65] Zhu, H., Yao, H. D., Ringsberg, J. W. (2024). Unsteady RANS and IDDES studies on a telescopic crescent-shaped wingsail. *Ships Offshore Struct.* 19, 134–147.
[66] Zhang, R., Huang, L. Z., Ma, R. Q., Peng, G. S., Ruan, Z., Wang, C., Zhao, H. Y., Li, B. Y., Wang, K. (2024). Numerical investigation on the effects of heel on the aerodynamic performance of wing sails. *Ocean Eng.* 305, 117897.
[67] Ma, Y., Bi, H. X., Hu, M. Q., Zheng, Y. Z., Gan, L. X. (2019). Hard sail optimization and energy efficiency enhancement for sail-assisted vessel. *Ocean Eng.* 173, 687–699.
[68] Chowdhury, J. I., Faieq, A., Amin, O. M. (2023). Seakeeping analysis of a tanker with hard sail-based wind propulsion system in various seaways. *Ocean Eng.* 278, 114481.
[69] He, J. H., Hu, Y. H., Tang, J. J., Xue, S. Y. (2015). Research on sail aerodynamics performance and sail-assisted ship stability. *J. Wind Eng. Ind. Aerodyn.* 146, 81–89.
[70] Wang, H. M., Li, C., Zuo, C. B., Yuan, J. F., Wu, B. X. (2024). Computational fluid dynamics investigation of the spacing of the aerodynamic characteristics for multiple wingsails on ships. *J. Mar. Sci. Eng.* 12, 985.
[71] Fang, S. P., Tian, C. W., Zhang, Y. Q., Xu, C. B., Ding, T. C., Wang, H. M., Xia, T. (2024). Aerodynamic analysis of rigid wing sail based on CFD simulation for the design of high-performance unmanned sailboats. *Mathematics* 12, 2481.
[72] Li, C., Wang, H. M., Sun, P. T. (2020). Numerical investigation of a two-element wingsail for ship auxiliary propulsion. *J. Mar. Sci. Eng.* 8, 333.
[73] Kawecki, B., Kulak, M., Lipian, M. (2024). Wing sails: numerical analysis of high-performance propulsion systems for a racing yacht. *Energies* 17, 549.
[74] Jiang, Y. X., Cao, C. Z., Cui, T., Yang, H., Tian, Z. J. (2024). Numerical study on auxiliary propulsion performance of foldable three-element Wingsail utilizing wind energy. *Energies* 17, 3833.
[75] Kuang, L. N., Li, H. Y., Su, X., Song, X., Wang, Z. S., Zhang, Y., Ma, W. Z. (2023). Effect of chord length ratio on aerodynamic performance of two-element wing sail. *Ocean Eng.* 287, 115946.
[76] Win, L. S. T., Win, S. K. H., Sufiyan, D., Foong, S. (2023). Novel rigid-wing bi-directional sailboat design and method of sailing. In *Proceedings of the 2023 IEEE/ASME International Conference on Advanced Intelligent Mechatronics (AIM)*. Seattle, USA, p 942–947.
[77] Makram, T. E., Panagiotou, P., Mattheou, D. (2023). Wingsail layout design and shape optimization using a CFD-aided Taguchi approach: the Aegean marathon case study. *Ocean Eng.* 276, 114055.
[78] Fujiwara, T., Hearn, G. E., Kitamura, F., Ueno, M. (2005). Sail–sail and sail–hull interaction effects of hybrid-sail assisted bulk carrier. *J. Mar. Sci. Technol.* 10, 82–95.
[79] Graf, K., Hoeve, A. V., Watin, S. (2014). Comparison of full 3D-RANS simulations with 2D-RANS/lifting line method calculations for the flow analysis of rigid wings for high performance multihulls. *Ocean Eng.* 90, 49–61.
[80] Viola, I. M., Sacher, M., Xu, J. S., Wang, F. (2015). A numerical method for the design of ships with wind-assisted propulsion. *Ocean Eng.* 105, 33–42.
[81] Li, Q., Nihei, Y., Nakashima, T., Ikeda, Y. (2015). A study on the performance of cascade hard sails and sail-equipped vessels. *Ocean Eng.* 98, 23–31.
[82] Paulig, X., Bungart, M., Specht, B. (2013). Conceptual design of textile kites considering overall system performance. In Airborne Wind Energy. Ahrens, U., Diehl, M., Schmehl, R., Eds. Berlin: Springer, p 547–562.
[83] Traut, M., Gilbert, P., Walsh, C., Bows, A., Filippone, A., Stansby, P., Wood, R. (2014). Propulsive power contribution of a kite and a Flettner rotor on selected shipping routes. *Appl. Energy* 113, 362–372.
[84] WASP. (2020). Preliminary results of North Sea Region WASP. https://northsearegion.eu/wasp/preliminary-results/. (accessed 22 July 2025).
[85] Chen, W. L., Wang, H. F., Liu, X. Y. (2023). Experimental investigation of the aerodynamic performance of Flettner rotors for marine applications. *Ocean Eng.* 281, 115006.
[86] Kwon, C. S., Yeon, S. M., Kim, Y. C., Kim, Y. G., Kim, Y. H., Kang, H. J. (2022). A parametric study for a flettner rotor in standalone condition using CFD. *Int. J. Naval Arch. Ocean Eng.* 14, 100493.
[87] Liu, J. H., Ma, W. Y., Zheng, D. Q., Jin, L. Q., Liu, Q. (2024). Numerical investigation of cylinder rotors with various endplates.

Phys. Fluids 36, 074101.
[88] Shiii, T., Yagi, H., Fujii, A. (2006). Wind Tunnel study of column-type circular cylinder propulsion assistance system (C-PAS) for ships. In *Proceedings of the Fourth International Symposium on Computational Wind Engineering*. Yokahama, Japan, p 673–676.
[89] Ghorbani, M. T., Slaets, P., Lacey, J. (2022). A numerical investigation of a wind-assisted ship to estimate fuel savings. In *Proceedings of the OCEANS 2022*. Chennai, India, p 1–10.
[90] Hcini, C., Abidi, E., Kamoun, B., Afungchui, D. (2017). A Turbosail profile analysis code based on the panel method. *Energy* 118, 147–155.
[91] Ghorbani, M., Slaets, P., Lacey, J. (2024). Sensor-based modelling of suction sails to integrate into a numerical simulation tool for a wind-assisted vessel and its application to green shipping. *Ocean Eng.* 311, 118937.
[92] Lee, H., Jo, Y., Lee, D. J., Choi, S. (2016). Surrogate model based design optimization of multiple wing sails considering flow interaction effect. *Ocean Eng.* 121, 422–436.
[93] Canale, M., Fagiano, L., Milanese, M. (2010). High altitude wind energy generation using controlled power kites. *IEEE Trans. Control Syst. Technol.* 18, 279–293.
[94] Fagiano, L., Milanese, M., Piga, D. (2012). Optimization of airborne wind energy generators. *Int. J. Robust Nonlinear Control* 22, 2055–2083.
[95] Trevisi, E., Gaunaa, M., Mcwilliam, M. (2020). The influence of tether sag on airborne wind energy generation. *J. Phys. Conf. Ser.* 1618, 032006.
[96] Fagiano, L., Quack, M., Bauer, F., Carnel, L., Oland, E. (2022). Autonomous airborne wind energy systems: accomplishments and challenges. *Annu. Rev. Control Rob. Auton. Syst.* 5, 603–631.
[97] Cherubini, A. (2011). Kite Dynamics and Wind Energy Harvesting. Master Degree Thesis. Politecnico di Milano, Milan, Italy.
[98] Lv, J. Z., Lin, Y. Q., Zhang, R., Li, B. Y., Yang, H. L. (2022). Assisted propulsion device of a semi-submersible ship based on the magnus effect. *Pol. Marit. Res.* 29, 33–46.
[99] Seo, J., Park, D. W. (2024). Numerical study on the aerodynamic performance of four flettner rotors by varying distance and spin ratio. *J. Mar. Sci. Technol.* 32, 2.
[100] Jiang, Y. L., Liu, K., Zhang, Q., Zhang, Z. (2024). Lift modeling, load and vibration analysis of Magnus rotors. *Ocean Eng.* 303, 117690.
[101] Kume, K., Hamada, T., Kobayashi, H., Yamanaka, S. (2022). Evaluation of aerodynamic characteristics of a ship with flettner rotors by wind tunnel tests and RANS-based CFD. *Ocean Eng.* 254, 111345.
[102] Argatov, I., Rautakorpi, P., Silvennoinen, R. (2011). Apparent wind load effects on the tether of a kite power generator. *J. Wind Eng. Ind. Aerodyn.* 99, 1079–1088.
[103] Vander Lind, D. (2013). Analysis and flight test validation of high performance airborne wind turbines. In Airborne Wind Energy. Ahrens, U., Diehl, M., Schmehl, R., Eds. Berlin: Springer, p 473–490.
[104] Bigi, N., Roncin, K., Leroux, J. B., Parlier, Y. (2020). Ship towed by kite: Investigation of the dynamic coupling. *J. Mar. Sci. Eng.* 8, 486.
[105] Zhou, B., Wang, X. K., Guo, W., Gho, W. M., Tan, S. K. (2015). Experimental study on flow past a circular cylinder with rough surface. *Ocean Eng.* 109, 7–13.
[106] Thom, A., Sengupta, S. R. (1933). Air Torque on a Cylinder Rotating in an Air Stream. London: HMSO.
[107] Hojo, T. (2015). Control of flow around a circular cylinder using a patterned surface. *WIT Trans. Modell. Simul.* 59, 245–256.
[108] Asrokin, A., Ramly, M. R., Ahmad, A. H. (2013). Rotating cylinder design as a lifting generator. *IOP Conf. Ser. Mater. Sci. Eng.* 50, 012025.
[109] Prince, S., Holt, J., Episkopou, P. (2016). Geometric roughness effects on the aerodynamic characteristics of a spinning cylinder in Crossflow. In *Proceedings of the 30th Congress of the International Council of the Aeronautical Sciences*. Daejeon, Korea, p 1–10.
[110] Lee, K., Kim, Y. H., Park, J., Choi, B., Kang, H. J. (2023). Preliminary feasibility study of a magnetic levitation rotor sail for coastal area operations. *J. Mar. Sci. Eng.* 12, 32.
[111] DNV (2023). DNV-ST-0511 Wind assisted propulsion systems. Report, DNV.
[112] BV (2025). NR206 wind propulsion systems. Report, BV.
[113] ABS (2022). Requirements for wind assisted propulsion system installation. Report, ABS.
[114] ClassNK (2023). Guidelines for wind-assisted propulsion systems for ships (Edition 2.0). Report, ClassNK.
[115] CCS (2023). Guidelines for survey of marine wind-rotor assisted propulsion system. Report, CCS.
[116] KR (2025). Guidance for prevention systems of pollution from ships, Chapter 5 wind assisted propulsion systems. Report, KR.
[117] Zhou, Y., Lu, P., Zhou, X., Bai, J. H., An, S. S., Liu, S. Z., Pu, X. J. (2024). Triboelectric wind sensors: fundamentals, progress, and perspectives. *Nano Energy* 131, 110209.
[118] Zou, Y. J., Sun, M. Z., Li, S., Zhang, X. Y., Feng, L., Wang, Y., Du, T. L., Ji, Y. L., Sun, P. T., Xu, M. Y. (2024). Advances in self-powered triboelectric sensor toward marine IoT. *Nano Energy* 122, 109316.
[119] Pezeshki, H., Adeli, H., Pavlou, D., Siriwardane, S. C. (2023). State of the art in structural health monitoring of offshore and marine structures. *Proc. Inst. Civil Eng. Marit. Eng.* 176, 89–108.
[120] Bordogna, G., Muggiasca, S., Giappino, S., Belloli, M., Keuning, J. A., Huijsmans, R. H. M. (2020). The effects of the aerodynamic interaction on the performance of two Flettner rotors. *J. Wind Eng. Ind. Aerodyn.* 196, 104024.
[121] Zhang, R., Huang, L. Z., Peng, G. S., Ruan, Z., Ma, R. Q., Wang, K., Cao, J. L., Wu, J. Y., Li, X. W. (2025). Investigation of aerodynamic performance and operational optimization of wing sails at varying spacings. *Ocean Eng.* 333, 121444.
[122] Tillig, F., Ringsberg, J. W. (2020). Design, operation and analysis of wind-assisted cargo ships. *Ocean Eng.* 211, 107603.
[123] Zhang, R., Huang, L. Z., Wang, K., Ma, R. Q., Ruan, Z., Wang, C. (2024). Novel optimized layout for Flettner rotors based on reuse of wake energy. *J. Cleaner Prod.* 443, 140922.
[124] Zhang, W. Z., Calderon-Sanchez, J., Duque, D., Souto-Iglesias, A. (2024). Computational fluid dynamics (CFD) applications in floating offshore wind turbine (FOWT) dynamics: a review. *Appl. Ocean Res.* 150, 104075.
[125] Peña, A., Gryning, S. E., Hasager, C. B. (2008). Measurements and modelling of the wind speed profile in the marine atmospheric boundary layer. *Bound. Layer Meteor.* 129, 479–495.
[126] Li, C., Wang, H. M., Sun, P. T. (2023). Study on the influence of gradient wind on the aerodynamic characteristics of a two-element wingsail for ship-assisted propulsion. *J. Mar. Sci. Eng.* 11, 134.
[127] Yeon, S., Kwon, C. S., Kim, Y. C., Kim, K. S., Kim, Y. G., Kim, Y. H., Kang, H. J. (2025). Performance analysis of Flettner rotor considering Marine wind profile and ship installation using CFD. *Int. J. Naval Archit. Ocean Eng.* 17, 100653.
[128] Zeng, X. M., Zhang, H. W. (2018). Experimental study of the aerodynamics of sail in natural wind. *Pol. Marit. Res.* 25, 17–22.
[129] Massaro, D., Karp, M., Jansson, N., Markidis, S., Schlatter, P. (2024). Direct numerical simulation of the turbulent flow around a Flettner rotor. *Sci. Rep.* 14, 3004.
[130] Bouhourd, C., Perret, L., Cossu, C. (2024). Wingsail performance in unsteady atmospheric surface layer winds. *Ocean Eng.* 314, 119653.
[131] Zeng, Q. S., Lyu, X., Cai, W., Zhang, L., Xu, J. H. (2024). Influence of wind gradient and ground effect on the aerodynamic forces of a Dynarig sail at large heeling angles. *Ocean Eng.* 312, 119069.
[132] Fujiwara, T., Hearn, G. E., Kitamura, F., Ueno, M., Minami, Y. (2005). Steady sailing performance of a hybrid-sail assisted bulk carrier. *J. Mar. Sci. Technol.* 10, 131–146.

[133] Copuroglu, H. I., Pesman, E. (2018). Analysis of Flettner rotor ships in beam waves. *Ocean Eng.* 150, 352–362.
[134] Sauder, T., Alterskjær, S. A. (2022). Hydrodynamic testing of wind-assisted cargo ships using a cyber–physical method. *Ocean Eng.* 243, 110206.
[135] Liu, S., Song, J., Zhang, L. Y. (2024). An adaptive bi-limit homogeneous sliding mode control for 3-DOF stabilized system of ship propulsion-assisted sail with prescribed performance. *Ocean Eng.* 302, 117624.
[136] Liu, S., Song, J., Zhang, L. Y. (2023). Research on 3-DOF stabilized control system of ship propulsion-assisting sail. *Ocean Eng.* 278, 114370.
[137] Liu, S., Song, J., Zhang, L. Y., Tan, Y. C. (2024). Adaptive finite-time backstepping integral sliding mode control of three-degree-of-freedom stabilized system for ship propulsion-assisted sail based on the inverse system method. *J. Mar. Sci. Eng.* 12, 348.
[138] Paik, J. K., Kim, B. J., Seo, J. K. (2008). Methods for ultimate limit state assessment of ships and ship-shaped offshore structures: Part I—unstiffened plates. *Ocean Eng.* 35, 261–270.
[139] Kujala, P., Goerlandt, F., Way, B., Smith, D., Yang, M., Khan, F., Veitch, B. (2019). Review of risk-based design for ice-class ships. *Mar. Struct.* 63, 181–195.
[140] Fricke, W., Kahl, A. (2005). Comparison of different structural stress approaches for fatigue assessment of welded ship structures. *Mar. Struct.* 18, 473–488.
[141] Zhang, W. Z., Pan, J., Sanchez, J. C., Li, X. B., Xu, M. C. (2024). Review on the protective technologies of bridge against vessel collision. *Thin-Walled Struct.* 201, 112013.
[142] Wang, L. K., Wang, J. H., Shi, M. Y., Fu, S. S., Zhu, M. (2021). Critical risk factors in ship fire accidents. *Marit. Policy Manage.* 48, 895–913.
[143] Pereira, T., Garbatov, Y. (2022). Multi-attribute decision-making ship structural design. *J. Mar. Sci. Eng.* 10, 1046.
[144] Malinoski, Z. J. (2002). An Approach for Structural Maintenance Scheduling Using Time Variant Reliability Analysis of Serviceability and Ultimate Strength Models. Master Degree Thesis. Massachusetts Institute of Technology, Cambridge, MA, USA.
[145] Kim, D. M., Hong, S. H., Jeong, S. H., Kim, S. J. (2024). Analysis of dynamic characteristics of rotor sail using a 4DOF rotor model and finite element model. *J. Mar. Sci. Eng.* 12, 335.
[146] Hu, R. Q., Wang, W. Z., Zhang, C. (2023). Effect of preloading on vibration and buckling responses of variable stiffness composite cylindrical shells. *Eng. Struct.* 287, 116193.
[147] Xia, Y. J., Dai, Y. T., Huang, G. J., Yang, C. (2024). Stall flutter mitigation of an airfoil by active surface morphing. *Phys. Fluids.* 36, 083612.
[148] Xia, Y. J., Huang, G. J., Dai, Y. T., Yang, C., Wu, Y. (2023). Mode transition in fluid–structure interaction of piezoelectric membrane wings. *Phys. Fluids* 35, 023609.
[149] Grifò, M., Gulizzi, V., Milazzo, A., Da Ronch, A., Benedetti, I. (2023). High-fidelity aeroelastic transonic analysis using higher-order structural models. *Compos. Struct.* 321, 117315.
[150] DNV (2024). DNV rules for ships Pt. 3 Ch. 4 Sec. 3. Report, DNV.
[151] Formosa, W., Sant, T., De Marco Muscat-Fenech, C., Figari, M. (2023). Wind-assisted ship propulsion of a series 60 ship using a static kite sail. *J. Mar. Sci. Eng.* 11, 117.
[152] Bordogna, G., Muggiasca, S., Giappino, S., Belloli, M., Keuning, J. A., Huijsmans, R. H. M., Van't Veer, A. P. (2019). Experiments on a Flettner rotor at critical and supercritical Reynolds numbers. *J. Wind Eng. Ind. Aerodyn.* 188, 19–29.
[153] Edwards, E. C., Barbour, E., Tosdevin, T., Ransley, E., Monk, K., Reynolds, A., Holcombe, A., Brown, S., Greaves, D., Hann, M. (2025). Scaled physical modelling of floating offshore wind turbines using a neural network-based surrogate model for aerodynamic emulation. *Wind Energy* 28, e70052.
[154] LR (2024). Guidance notes on wind assisted propulsion systems. Report, LR.
[155] Zis, T. P. V., Psaraftis, H. N., Ding, L. (2020). Ship weather routing: a taxonomy and survey. *Ocean Eng.* 213, 107697.
[156] Grifoll, M., Borén, C., Castells-Sanabra, M. (2022). A comprehensive ship weather routing system using CMEMS products and A* algorithm. *Ocean Eng.* 255, 111427.
[157] Vettor, R., Soares, C. G. (2016). Development of a ship weather routing system. *Ocean Eng.* 123, 1–14.
[158] Chen, Y. H., Zhang, C., Guo, Y. H., Wang, Y. Y., Lang, X., Zhang, M. Y., Mao, W. G. (2025). State-of-the-art optimization algorithms in weather routing—ship decision support systems: challenge, taxonomy, and review. *Ocean Eng.* 331, 121198.
[159] Bentin, M., Zastrau, D., Schlaak, M., Freye, D., Elsner, R., Kotzur, S. (2016). A new routing optimization tool-influence of wind and waves on fuel consumption of ships with and without wind assisted ship propulsion systems. *Transp. Res. Procedia* 14, 153–162.
[160] Sun, W. Y., Tang, S. Y., Liu, X. Y., Zhou, S. N., Wei, J. F. (2022). An improved ship weather routing framework for CII reduction accounting for wind-assisted rotors. *J. Mar. Sci. Eng.* 10, 1979.
[161] Guzelbulut, C., Badalotti, T., Suzuki, K. (2025). Impact of control strategies for wind-assisted ships on energy consumption. *Brodogradnja* 76, 76104.
[162] Guzelbulut, C., Badalotti, T., Fujita, Y., Sugimoto, T., Suzuki, K. (2024). Artificial neural network-based route optimization of a wind-assisted ship. *J. Mar. Sci. Eng.* 12, 1645.
[163] Liu, X., Wang, K., Guo, X., Li, Z. W., Wu, J. Y., Ma, R. Q., Huang, L. Z., Li, X. W. (2025). An integrated energy efficiency optimization method of the wind-assisted hybrid ship for the shipping decarbonization. *Mar. Pollut. Bull.* 212, 117579.
[164] Öztürk, Ü., Akdağ, M., Ayabakan, T. (2022). A review of path planning algorithms in maritime autonomous surface ships: navigation safety perspective. *Ocean Eng.* 251, 111010.
[165] Wu, C. B., Yu, W. N., Li, G. Z., Liao, W. Q. (2023). Deep reinforcement learning with dynamic window approach based collision avoidance path planning for maritime autonomous surface ships. *Ocean Eng.* 284, 115208.
[166] Li, G. S., Zhang, X. K. (2022). Research on the influence of wind, waves, and tidal current on ship turning ability based on Norrbin model. *Ocean Eng.* 259, 111875.
[167] Zhao, H. Y., Huang, L. Z., Ma, R. Q., Wang, K., Wang, T. C., Ruan, Z., Zhang, R., Jiang, B. S., Li, X. W., Wu, J. Y. (2024). Dynamic nonparametric modeling of sail-assisted ship maneuvering motion based on GWO-KELM. *Ocean Eng.* 312, 119060.
[168] Hirano, M., Takashina, J. (1980). A calculation of ship turning motion taking coupling effect due to heel into consideration. *Tran. West Jpn. Soc. Naval Archit.* 59, 71–81.
[169] Ogawa, A., Koyama, T., Kijima, K. (1977). MMG report-I, on the mathematical model of ship manoeuvring. *Bull. Soc. Naval Archit. Jpn.* 575, 22–28.
[170] Yasukawa, H., Yoshimura, Y. (2015). Introduction of MMG standard method for ship maneuvering predictions. *J. Mar. Sci. Technol.* 20, 37–52.
[171] Kijima, K., Katsuno, T., Nakiri, Y., Furukawa, Y. (1990). On the manoeuvring performance of a ship with theparameter of loading condition. *J. Soc. Naval Archit. Jpn.* 1990, 141–148.
[172] Yang, X. D., Wang, H. D., Zhang, R. T., Sun, S. P, Zhang, M. Y. (2026). A deep learning method for spatiotemporal significant wave height estimation with ship attitude compensation. *Ocean Eng.* 352, 124517.
[173] Arabnejad, M. H., Thies, F., Yao, H. D., Ringsberg, J. W. (2024). Zero-emission propulsion system featuring, flettner rotors, batteries and fuel cells, for a merchant ship. *Ocean Eng.* 310, 118618.
[174] Ammar, N. R., Seddiek, I. S. (2025). Enhancing sustainability in LNG carriers through integrated alternative propulsion systems with Flettner rotor assistance. *Brodogradnja* 76, 76102.
[175] Alkhaledi, A. N., Sampath, S., Pilidis, P. (2023). Techno

environmental assessment of Flettner rotor as assistance propulsion system for LH2 tanker ship fuelled by hydrogen. *Sustain. Energy Technol. Assess.* 55, 102935.

[176] Nyanya, M. N., Vu, H. B., Schönborn, A., Ölçer, A. I. (2021). Wind and solar assisted ship propulsion optimisation and its application to a bulk carrier. *Sustain. Energy Technol. Assess.* 47, 101397.

[177] Julià, E., Tillig, F., Ringsberg, J. W. (2020). Concept design and performance evaluation of a fossil-free operated cargo ship with unlimited range. *Sustainability* 12, 6609.

[178] Thies, F., Ringsberg, J. W. (2023). Wind-assisted, electric, and pure wind propulsion–the path towards zero-emission RoRo ships. *Ships Offshore Struct.* 18, 1229–1236.

[179] Zhang, G. Q., Li, J. Q., Chang, T. Y., Zhang, W. J., Song, L. (2025). Autonomous navigation and control for a sustainable vessel: a wind-assisted strategy. *Sustain. Horiz.* 13, 100117.

[180] Vigna, V., Figari, M. (2023). Wind-assisted ship propulsion: matching flettner rotors with diesel engines and controllable pitch propellers. *J. Mar. Sci. Eng.* 11, 1072.

[181] Wang, Z., Chen, L., Huang, L. Z., Wang, K., Ma, R. Q., Wang, B. (2025). A novel multivariable coupling optimization method of wind-assisted propulsion system for a large crude carrier. *Energy* 322, 135720.

[182] Lan, T., Huang, L. Z., Ruan, Z., Cao, J. L., Ma, R. Q., Wu, J. Y., Li, X. W., Chen, L., Wang, K. (2025). Multilevel parallel integration framework for enhancing energy efficiency of wing-assisted ships based on deep learning and intelligent algorithms: towards a smarter and greener shipping. *Appl. Energy* 394, 126202.

[183] Wang, K., Guo, X., Zhao, J. H., Ma, R. Q., Huang, L. Z., Tian, F., Dong, S. Y., Zhang, P., Liu, C. L., Wang, Z. (2022). An integrated collaborative decision-making method for optimizing energy consumption of sail-assisted ships towards low-carbon shipping. *Ocean Eng.* 266, 112810.

[184] Chica, M., Hermann, R. R., Lin, N. (2023). Adopting different wind-assisted ship propulsion technologies as fleet retrofit: an agent-based modeling approach. *Technol. Forecast. Soc. Change* 192, 122559.

[185] Zhang, P. F., Lozano, J., Wang, Y. F. (2021). Using Flettner rotors and Parafoil as alternative propulsion systems for bulk carriers. *J. Cleaner Prod.* 317, 128418.

[186] Malmek, K., Larsson, L., Werner, S., Ringsberg, J. W., Bensow, R., Finnsgård, C. (2024). Rapid aerodynamic method for predicting the performance of interacting wing sails. *Ocean Eng.* 293, 116596.

[187] Reche-Vilanova, M., Hansen, H., Bingham, H. B. (2021). Performance prediction program for wind-assisted cargo ships. *J. Sailing Technol.* 6, 91–117.

[188] Talluri, L., Nalianda, D. K., Giuliani, E. (2018). Techno economic and environmental assessment of Flettner rotors for marine propulsion. *Ocean Eng.* 154, 1–15.

[189] Lindstad, E., Polić, D., Rialland, A., Sandaas, I., Stokke, T. (2022). Decarbonizing bulk shipping combining ship design and alternative power. *Ocean Eng.* 266, 112798.

[190] Angelini, G., Muggiasca, S., Belloli, M. (2023). A techno-economic analysis of a cargo ship using flettner rotors. *J. Mar. Sci. Eng.* 11, 229.

[191] Ghorbani, M., Slaets, P., Lacey, J. (2023). A numerical simulation tool for a wind-assisted vessel verified with logged data at sea. *Ocean Eng.* 290, 116319.

[192] Ma, R. Q., Wang, Z. Y., Wang, K., Zhao, H. Y., Jiang, B. S., Liu, Y. Z., Xing, H., Huang, L. Z. (2023). Evaluation method for energy saving of sail-assisted ship based on wind resource analysis of typical route. *J. Mar. Sci. Eng.* 11, 789.

[193] Reche-Vilanova, M., Bingham, H. B., Fluck, M., Morris, D., Psaraftis, H. N. (2024). Propeller and engine performance of commercial windships: benefits and trade-offs. *J. Ship Res.* 68, 1–15.

[194] Čalić, A., Jurić, Z., Katalinić, M. (2024). Impact of wind-assisted propulsion on fuel savings and propeller efficiency: a case study. *J. Mar. Sci. Eng.* 12, 2100.

[195] Guzelbulut, C., Sugimoto, T., Fujita, Y., Suzuki, K. (2024). Investigation of the efficiency of wind-assisted systems using model-based design approach. *J. Mar. Sci. Technol.* 29, 387–403.

[196] Tillig, F., Ringsberg, J., Psaraftis, H., Zis, T. (2019). ShipCLEAN–an integrated model for transport efficiency, economics and CO_2 emissions in shipping. In *Proceedings of the 2nd International Conference on Modelling an Oprimisation of Ship Energy Systems (MOSES2019)*. Glasgow, UK, p 189–198.

[197] Thies, F., Ringsberg, J. W. (2025). Sea trials vs prediction by numerical models—uncertainties in the measurements and prediction of wasp performance. *J. Ocean Eng. Sci.* 10, 239–245.

[198] Tillig, F., Ringsberg, J. W., Psaraftis, H. N., Zis, T. (2020). Reduced environmental impact of marine transport through speed reduction and wind assisted propulsion. *Transp. Res. Part D: Transp. Environ.* 83, 102380.

[199] Thies, F., Ringsberg, J. W. (2023). Retrofitting WASP to a RoPax vessel—design, performance and uncertainties. *Energies* 16, 673.

[200] Tillig, F., Ringsberg, J. W. (2019). A 4 DOF simulation model developed for fuel consumption prediction of ships at sea. *Ships Offshore Struct.* 14, 112–120.

[201] Psaraftis, H. N. (2019). Speed optimization for sustainable shipping. In Sustainable Shipping: A Cross-Disciplinary View. Cham, Germany, p 339–374.

[202] ENERCON (2013). Product pick of the week-Enercon's rotor sail ship E-ship 1 saves up to 25% fuel. https://w3.windfair.net/wind-energy/news/13639-product-pick-of-theweek-enercon-s-rotor-sail-ship-e-ship-1-saves-up-to-25-fuel. (accessed 14 July 2025).

[203] Norsepower, Norsepower's Rotor Sail solution on board Bore's mv Estraden. (2019). https://spliethoff-group.foleon.com/spliethoff-group-sustainability-report/spliethoff-group-sustainability-report-edition-1/norsepower-rotor-sail-onboard-mv-estraden (accessed 14 July 2025).

[204] Werner, S., Nisbet, J. (2023). Speed trial and route analysis of m/v Copenhagen with Flettner rotor. Report, SSPA.

[205] Norsepower (2019). Norsepower Rotor Sails confirmed savings of 8.2% fuel and associated CO_2 in Maersk Pelican project. https://www.norsepower.com/post/norsepower-rotor-sails-confirmed-savings-of-8-2-fuel-and-associated-co2-in-maersk-pelican-project/. (accessed 14 July 2025).

[206] Werner, S. (2022). Speed trial and route analysis of m/v Annika Braren with rotor sail. Report, SSPA.

[207] Cargill (2024). Cargill shares outcome of the world's first wind-powered ocean vessel's maiden voyage. https://www.cargill.com/2024/first-wind-powered-ocean-vessel-maiden-voyage. (accessed 14 July 2025).

[208] Jallal, C. (2023). Berge Olympus: the most powerful sailing cargo ship in the world. https://www.rivieramm.com/news-content-hub/news-content-hub/berge-olympus---the-most-powerful-sailing-cargo-ship-in-the-world-78142. (accessed 14 July 2025).

[209] Werner, S. (2022). Speed trial and route analysis of m/v Frisian Sea with suction wings. Report, SSPA.

[210] bound4blue (2025). bound4blue hits bullseye with third-party assessed average daily fuel savings of 1.7 metric tons, and higher peaks, on LDA ro-ro. https://bound4blue.com/bound4blue-hits-bullseye-with-third-party-assessed-average-daily-fuel-savings-of-1-7-metric-tons/. (accessed 14 July 2025).

[211] Wikipedia. MS Onego Deusto. (2019). https://en.wikipedia.org/wiki/MS_Onego_Deusto. (accessed 14 July 2025).

[212] Sheikh, N. J., Kocaoglu, D. F., Lutzenhiser, L. (2016). Social and political impacts of renewable energy: Literature review. *Technol. Forecast. Soc. Change* 108, 102–110.

[213] Maketo, L., Ashworth, P. (2025). Social acceptance of green hydrogen in European Union and the United Kingdom: a systematic review. *Renew. Sustain. Energy Rev.* 218, 115827.

[214] Buchner, J., Menrad, K., Decker, T. (2025). Public acceptance of green hydrogen production in Germany. *Renew. Sustain. Energy Rev.*

208, 115057.
[215] Hornung, J. (2023). Social identities and deadlocked debates on nuclear energy policy. *J. Eur. Public Policy* 30, 1911–1935.
[216] Jang, Y., Park, E. (2020). Social acceptance of nuclear power plants in Korea: the role of public perceptions following the Fukushima accident. *Renew. Sustain. Energy Rev.* 128, 109894.
[217] Kauschke, L., Vogt, J. (2025). Increasing public acceptance of fuel cell vehicles in Germany: a perspective on pioneer users. *Int. J. Hydrogen Energy* 148, 149726.
[218] Enevoldsen, P., Sovacool, B. K. (2016). Examining the social acceptance of wind energy: Practical guidelines for onshore wind project development in France. *Renew. Sustain. Energy Rev.* 53, 178–184.
[219] Hübner, G., Leschinger, V., Müller, F. J. Y., Pohl, J. (2023). Broadening the social acceptance of wind energy–an integrated acceptance model. *Energy Policy* 173, 113360.
[220] Jiang, Z. Y. (2025). Mooring design for floating wind turbines: a review. *Renew. Sustain. Energy Rev.* 212, 115231.
[221] Edwards, E. C., Holcombe, A., Brown, S., Ransley, E., Hann, M., Greaves, D. (2023). Evolution of floating offshore wind platforms: a review of at-sea devices. *Renew. Sustain. Energy Rev.* 183, 113416.
[222] Rako-Gospić, N., Picciulin, M. (2019). Underwater noise: Sources and effects on marine life. In World Seas: An Environmental Evaluation. 2nd ed. Sheppard, C., Ed. Amsterdam: Elsevier, p 367–389.
[223] Erbe, C., Marley, S. A., Schoeman, R. P., Smith, J. N., Trigg, L. E., Embling, C. B. (2019). The effects of ship noise on marine mammals—a review. *Front. Mar. Sci.* 6, 606.
[224] Ballini, F., Ölçer, A. I., Brandt, J., Neumann, D. (2017). Health costs and economic impact of wind assisted ship propulsion. *Ocean Eng.* 146, 477–485.
[225] Lam, J. S. L., Li, K. X. (2019). Green port marketing for sustainable growth and development. *Transp. Policy* 84, 73–81.
[226] Hossain, K. A., Zakaria, N. M. G. (2017). A study on global shipbuilding growth, trend and future forecast. *Procedia Eng.* 194, 247–253.
[227] Romero, E., Chica, M., Hermann, R. R., Damas, S. (2025). Targeting incentives to adopt wind-assisted technologies in shipping by agent-based simulations. *Transp. Res. Part D: Transp. Environ.* 138, 104511.
[228] Karslen, R., Papachristos, G., Rehmatulla, N. (2019). An agent-based model of climate-energy policies to promote wind propulsion technology in shipping. *Environ. Innovation Soc. Transitions* 31, 33–53.
[229] Searcy, T. (2017). Harnessing the wind: A case study of applying Flettner rotor technology to achieve fuel and cost savings for Fiji's domestic shipping industry. *Mar. Policy* 86, 164–172.
[230] Chen, S. Y., Hao, S. T., Meng, B., Zhang, Y. J., Kuang, H. B. (2025). Revisiting oil and tanker shipping markets: the role of geopolitical risk in shaping spillover dynamics. *Energy* 321, 135494.
[231] Yap, W. Y., Yang, D. (2024). Geopolitical tension and shipping network disruption: analysis of the red sea crisis on container port calls. *J. Transp. Geogr.* 121, 104004.
[232] Marobhe, M. I., Kansheba, J. M., Munim, Z. H. (2025). Geopolitical uncertainty and shipping stock returns: an event study of the Israel-Hamas conflict. *J. Transp. Geogr.* 123, 104122.